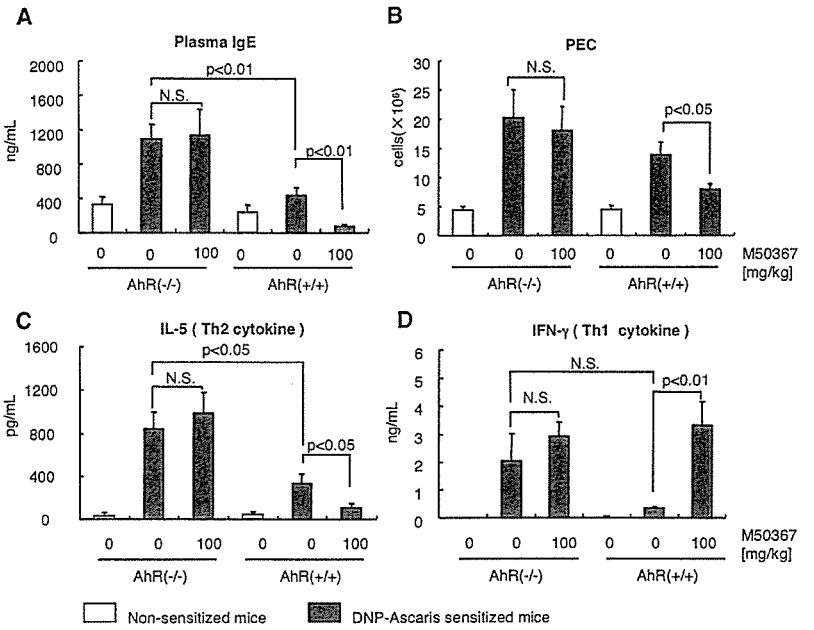

FIGURE 3. Effects of M50367 in in vivo allergic models using $AhR^{-/-}$ and wt mice sensitized with DNP-*Ascaris*. *A*, $AhR^{-/-}$ and wt mice sensitized with 10 μg of DNP-*Ascaris* were given 100 mg/kg M50367 orally. Ten days later, we assessed the IgE concentrations present in plasma samples collected on day 10 by mouse IgE ELISA. *B*, Mice were given 10 μg of DNP-*Ascaris* on day 0. This injection was repeated on day 7; the sensitized mice were treated orally from days 0 to 9 with 100 mg/kg M50367. On day 10, we measured the total number of peritoneal cells collected. *C* and *D*, $AhR^{-/-}$ and wt mice sensitized with 10 μg of DNP-*Ascaris* were given 100 mg/kg M50367 orally for 10 days. On day 10, isolated splenocytes were cultured at 5×10^6 cells/ml in the presence of 10 μg/ml DNP-*Ascaris* in the absence of M50367 for 18 h. We then estimated the concentrations of cytokines present in the supernatants by ELISA. Values are expressed as the means ± SEM of eight animals. $p < 0.05$; $p < 0.01$, calculated by the Student t comparison test.

harvesting the cells at various time points after stimulation, cell lysates were prepared for immunoblot analysis. AhR expression was strongly induced at the earliest time point, and then gradually decreased over the next 72 h (Fig. 5).

To confirm the modulation of Th1/Th2 differentiation by activated AhR, we investigated the effects of a CA-AhR on naive Th cells. Deletion of the ligand-binding domain (PAS B domain) converts AhR into a constitutively active molecule, even in the absence of ligand (15). The CA-AhR and wt-AhR expression vectors were constructed as described in *Materials and Methods* (Fig. 6*A*). After stimulation with anti-CD3 and anti-CD28 mAbs, naive Th cells from $AhR^{-/-}$ mice were infected with a retrovirus encoding wt-AhR or CA-AhR. Cells were cultured in the presence of exogenous IL-4 (10 ng/ml), and then the populations of Th1 and Th2 cells were assessed on day 6 (Fig. 6*B*). Despite the presence of exogenous IL-4, CA-AhR expression induced significant Th1 polarization (3.6–8.8%) with a concomitant decrease in Th2 differentiation (38.5–16.7%). In contrast, wt-AhR transduction did not significantly affect Th1/Th2 differentiation, indicating that activation of AhR modulates Th1/Th2 differentiation toward Th1 dominance.

We examined the modulatory effects of representative AhR ligands on Th cell differentiation. Naive Th cells isolated from wt C57BL/6 mice were stimulated with anti-CD3 and anti-CD28 mAbs in the presence of one of the following compounds: 3MC and βNF as AhR agonists, αNF as a partial antagonist, and resveratrol as a complete antagonist. We assessed the Th1 and Th2 cell populations by intracellular cytokine staining with flow cytometry on day 6 (Fig. 6*C*). M50354, 3MC, and βNF suppressed Th2 differentiation (from 16.2 to 8.0, 9.5, and 7.6%, respectively) with concomitant increases in Th1 differentiation (from 21.3 to 25.7, 23.6, and 25.1%, respectively), whereas αNF did not affect Th1/Th2 differentiation. Resveratrol treatment increased both the Th1 and Th2 populations, similar to the result observed in the Ag-sensitized $AhR^{-/-}$ mice. This result indicates that immunological responses following AhR antagonist treatment mimic the AhR deficiency status of mice. The estimated IC_{50} value of M50354 (~3 μM), βNF (~3 μM), and αNF (> 10 μM) for the inhibition of IL-4 production (Fig. 6*D*) did not agree with the observed EC_{50} for the induction of CYP1A1 expression (Fig. 2*A*), suggesting that AhR uses different molecular mechanisms in these processes.

Effects of M50354 on expression of genes in Th cell differentiation

Taken together with the result that M50354 treatment and CA-AhR transduction of naive Th cells suppressed Th2 differentiation, even in the presence of excess exogenous IL-4 (Ref. 13 and Fig. 6*B*), we presumed that the effect of AhR on Th1/Th2 differentiation likely occurs through modulation of a signaling component upstream of IL-4 action, such as GATA-3 or c-maf. GATA-3 is a master transcriptional factor controlling the differentiation of Th2 cells; impairment of GATA-3 activity by either antisense RNA or a dominant-negative form of the protein potently suppressed Th2 cytokine production and Th2 cell differentiation (26).

To test our hypothesis, we compared the expression of *GATA-3* in $AhR^{-/-}$ mice with that observed in the wt animals. Naive Th cells from $AhR^{-/-}$ and wt littermate mice were stimulated with anti-CD3 and anti-CD28 mAbs. Using RNAs prepared from these cells 24 h after stimulation, we measured the mRNA levels of *GATA-3* and other transcription factors by quantitative RT-PCR (Fig. 7*A*). *GATA-3* expression in naive Th cells isolated from $AhR^{-/-}$ mice exhibited ~3-fold higher GATA-3 mRNA levels than cells derived from wt mice, while the levels of *IL-4Rα*-chain and *STAT6* mRNA were not affected.

From these observations, we hypothesized that the suppression of *GATA-3* expression by activated AhR modulated Th1/Th2 differentiation. Thus, we examined the effect of M50354 on the time course of *GATA-3* mRNA expression. Naive Th cells isolated from C57BL/6 mice were stimulated with anti-CD3 and anti-CD28 mAbs in the presence or absence of M50354. At various time points after treatment, we used quantitative RT-PCR to measure the mRNA levels of *GATA-3* and other transcription factors within RNA samples prepared from these Th cells (Fig. 7*B*). In the absence of M50354, expression of *GATA-3* mRNA began to increase at 48 h, continuing to increase throughout the course of the experiment until 96 h. In the presence of M50354, however, *GATA-3* mRNA expression was already suppressed at 48 h, remaining low at ~10% of control levels at 96 h. mRNA expression levels of *c-maf* and *T-bet* were similarly increased in either the presence or absence of M50354. IL-4 protein production, quantitated by ELISA, began to increase at 72 h in untreated controls; M50354

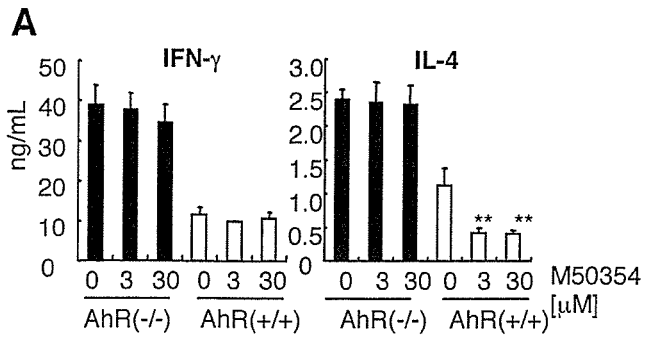

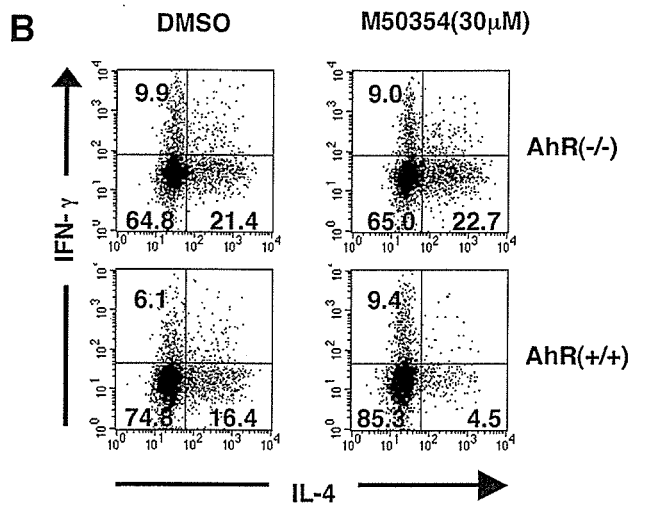

FIGURE 4. Effect of M50354 on the in vitro differentiation of naive Th cells of $AhR^{-/-}$ and wt mice into Th1 and Th2 cells. Naive Th cells prepared from $AhR^{-/-}$ or wt mice were stimulated with immobilized anti-CD3 (5 μg/ml) and anti-CD28 (1 μg/ml) mAbs, then cultured with 3 μm or 30 μM M50354. *A*, On day 3, culture supernatants were harvested; the levels of IL-4 and IFN-γ in these samples were determined by ELISA. Values are expressed as the means ± SD of four independent experiments. **, $p < 0.01$, calculated by Dunnett's procedure for multiple comparisons. *B*, On day 6, cells were restimulated with anti-CD3 mAb in the presence of monensin for 6 h. The proportions of IL-4- and IFN-γ-producing cells were then determined by intracellular cytokine staining, as described in *Materials and Methods*. The percentages of cells present in each quadrant are indicated.

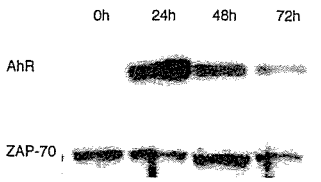

FIGURE 5. Time course of AhR expression during the in vitro differentiation of naive T cells. Naive Th cells prepared from C57BL/6 mice were costimulated with immobilized anti-CD3 (5 μg/ml) and anti-CD28 (1 μg/ml) mAbs. After 24, 48, and 72 h, cells were harvested and analyzed for the expression of AhR proteins by Western blotting using a specific anti-AhR Ab. The image shown is representative of three independent experiments.

treatment reduced these levels to 30% of the observed control levels. These results suggest that M50354 skewed Th1/Th2 differentiation toward Th1 dominance by inhibiting the expression of *GATA-3* in naive Th cells.

Discussion

Recently, there have been an increasing number of reports detailing the various effects of AhR signaling on the immune system, including thymic atrophy and suppression of Ab production, by an AhR ligand, TCDD. Thymic atrophy has been observed in several experimental animal models following exposure to TCDD, reportedly due to the direct effect of TCDD on thymocytes and lymphocyte precursors (27). Furthermore, TCDD exposure suppresses Ag-specific Ab production in mouse models (28, 29). Kerkvliet et al. (30) have also described the marked suppression of CTL responses following TCDD exposure. All of these effects of TCDD have been confirmed to be mediated by AhR signaling by experiments using AhR-deficient mice. These results strongly suggest that AhR is expressed in the T lineage cells, likely functioning in their differentiation and effector function.

The synthetic compound M50367 modulates the Th1/Th2 balance by influencing Th cell differentiation from naive T cells, resulting in the suppression of IgE production and eosinophilic infiltration into sites of inflammation in an in vivo allergy model (12, 13). The modulatory effect of M50354 on Th1/Th2 differentiation from naive Th cells is unique; to our knowledge, there have not been any previous reports detailing the effect of a small molecule, such as this chemical, on the modulation of the Th1/Th2 balance. Therefore, elucidating the mechanism of M50354 action would greatly contribute to our understanding of the mechanisms underlying Th1/Th2 differentiation, potentially facilitating the development of novel antiallergic agents. In this study, we demonstrate that the antiallergic compound M50354 bound and activated AhR, enhancing the expression of a reporter gene driven by the CYP1A1 promoter in transient DNA-transfection assays, gel mobility shift assays, and ligand-binding experiments. We also revealed that M50354 exerted inhibitory effects on Th2 cell differentiation and IgE production in both in vitro and in vivo experiments. As M50354 also suppressed the production of Th2 cytokines, including IL-4 and IL-5, the inhibition of IgE production by M50354 was likely caused by suppression of the differentiation of naive Th cells into Th2 cells, leading to a reduced production of Th2 cytokines. Although the inhibitory effects of this chemical were completely lost in $AhR^{-/-}$ mice, retroviral CA-AhR expression potently inhibited naive Th cell differentiation into Th2 cells in both $AhR^{-/-}$ and wt mice (data not shown), even in the presence of exogenous IL-4. These results indicate that M50354 suppressed Th2 cell differentiation from naive Th cells via activation of AhR signaling, exerting antiallergic effects. 3MC and βNF, representative AhR ligands, also inhibited naive T cell differentiation into Th2 cells and the production of the Th2 cytokines. These findings clearly indicate that AhR signaling regulates the Th1/Th2 balance by influencing Th cell differentiation. The potency of these chemicals to induce *CYP1A1* expression, however, differs from their immunomodulatory activities. M50354 exerted a greater immunomodulatory activity than the examined representative AhR ligands, βNF and 3MC, while the opposite was true for *CYP1A1* induction. Judging from the IC_{50} (~3 μM) for Th2 differentiation and the IC_{50} (> 300 μM) for *CYP1A1* induction, M50354 is specifically more effective in comparison to other AhR ligands at modulating Th cell differentiation than inducing CYP1A1 expression. The conformation of the AhR complex when bound to M50354 may differ from that bound to other AhR ligands. The molecular basis for the differential activities of these AhR ligands will be intriguing to investigate. TCDD, a high affinity AhR ligand, exerts pleiotropic immunosuppressive effects on the production of various Ab isotypes (IgE, IgG1, IgG2, and IgM) (31) and cytokines (IL-2,

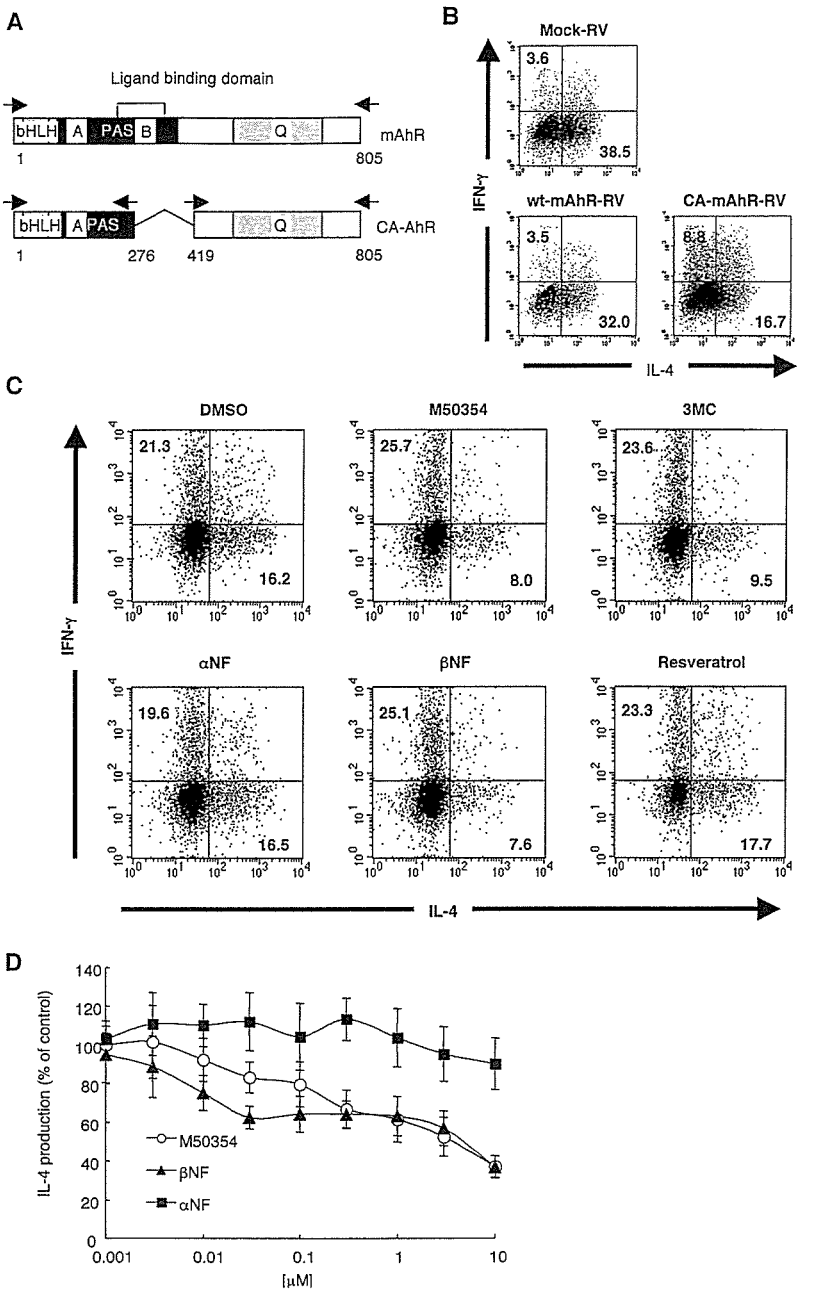

FIGURE 6. Effects of AhR signaling on in vitro Th1/Th2 differentiation. *A*, Schematic representation of the wt AhR and CA-AhR constructs. Q, glutamine rich domain. The positions of the primers used in the plasmid construction are indicated by arrows. *B*, The effects of CA-AhR transduction on Th1/Th2 differentiation. Naive Th cells prepared from $AhR^{-/-}$ mice were stimulated with immobilized anti-CD3 and anti-CD28 mAbs in the presence of IL-4. Cells were then infected with retroviruses encoding the wt AhR, CA-AhR, or control sequences at 24 and 72 h after stimulation. On day 6, cells were harvested and restimulated with anti-CD3 and anti-CD28 mAbs in the presence of monensin. Six hours later, cells were harvested to determine the proportions of IL-4- and IFN-γ-producing cells by intracellular cytokine staining, as described in the *Materials and Methods*. The percentages of cells present in each quadrant are indicated. *C*, Effects of AhR agonists and antagonists on Th1/Th2 differentiation. Naive Th cells prepared from C57BL/6 mice were stimulated with anti-CD3 and anti-CD28 mAbs in the presence of each AhR ligand (3 μM). Six days after stimulation, the cells were collected and restimulated with anti-CD3 and anti-CD28 mAbs in the presence of monensin. Six hours later, cells were harvested to determine the proportions of IL-4- and IFN-γ-producing cells by intracellular cytokine staining. The percentages of the cells present in each quadrant are indicated. *D*, Dose-dependent effect of each chemical on IL-4 production. Naive Th cells prepared from C57BL/6 mice were stimulated with anti-CD3 and anti-CD28 mAbs in the presence of varying concentrations of the indicated chemicals. On day 3, culture supernatants were harvested. The levels of IL-4 were then determined by ELISA. Values are expressed as the means ± SD of four experiments.

IL-4, IL-5, and IL-6). The majority of the effects of TCDD effects, if not all, are thought to be mediated by AhR. In contrast, M50367 did not affect the production of IgG2a, IgM, IL-2, or IL-6; its effects appear to be limited to Th2-mediated immune responses (12). Although M50364 treatment suppressed the expression of *GATA-3*, a key transcription factor for Th2 cell differentiation, it is not known whether activated AhR is directly involved in *GATA-3* expression. As the molecular mechanisms underlying T cell-specific *GATA-3* expression are complex and difficult to investigate (32), we are now investigating the mechanism of *GATA-3* expression inhibition by activated AhR. In the AhR-deficient mice, plasma IgE levels were significantly increased in comparison to those observed in wt mice; the production of both IL-5 and IFN-γ was 2- to 3-fold higher in the primary cultures of $AhR^{-/-}$ Th cells than that seen in wt animals. In AhR-deficient mice, the populations of both Th1 and Th2 cells were increased. Moreover, treatment with resveratrol, an AhR antagonist, enhanced cytokine production in a manner similar that seen in $AhR^{-/-}$ mice. These results indicate that AhR suppresses immune responses under normal conditions; ablation of AhR activity by either gene disruption or antagonist treatment also enhances immune responses. In the first description of AhR-deficient mice, Gonzalez and colleagues (33) reported a decreased accumulation of lymphocytes in the spleen and the lymph nodes, suggesting the requirement for AhR in the development of the immune system. In contrast, Kerkvliet and colleagues (34) reported that AhR-deficient mice generate normal immune responses in Ag-stimulation models. The apparent discrepancies between these results may result from differences in either the mouse stains or the methods used. More extensive analyses using a variety of immunological parameters and analytical methods should be performed to clarify these apparent discrepancies.

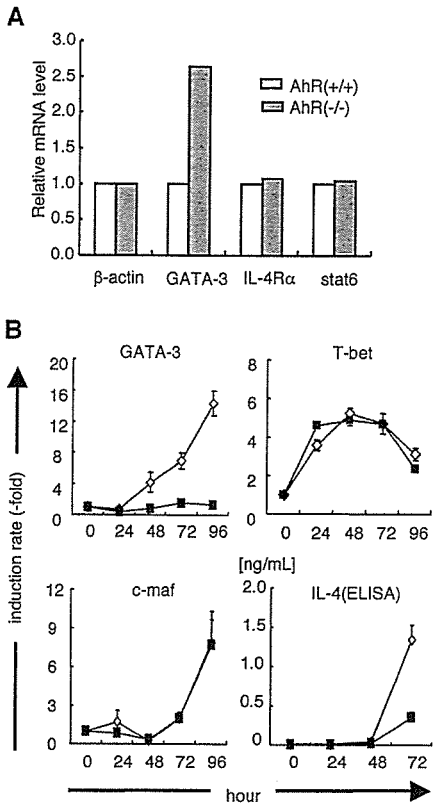

FIGURE 7. Effects of AhR signaling and M50354 treatment on *GATA-3* expression. *A*, Naive Th cells prepared from $AhR^{-/-}$ or wt mice were stimulated with immobilized anti-CD3 (5 μg/ml) and anti-CD28 (1 μg/ml) mAbs. After 24 h, cells were harvested and analyzed for gene expression by quantitative RT-PCR using an ABI7000 analyzer. Data are normalized to the expression levels of each gene in $AhR^{+/+}$ mice. *B*, Naive Th cells prepared from C57BL/6 mice were stimulated with immobilized anti-CD3 (5 μg/ml) and anti-CD28 (1 μg/ml) mAbs in the presence of either vehicle alone (diamonds) or M50354 (squares). After 72 h of culture, cells were expanded 6-fold in fresh medium, then cultured for an additional day. After 24, 48, 72, and 96 h of culture, the harvested cells were analyzed for gene expression by quantitative RT-PCR. Data are normalized to *β-actin* mRNA expression level. The means ± SD of triplicate determinations are shown.

Concerning the role of AhR signaling in the human immune system, Weisglas-Kuperus et al. (35) have reported that perinatal exposure to polychlorinated biphenyls (PCBs) and dioxins is associated with a lower prevalence of allergic diseases in preschool age children. These authors suggested that the lower prevalence is due to the susceptibility to infectious diseases in infants. Taken together with our results, the combined effects of infectious diseases and Th1-dominated conditions caused by exposure to PCBs and dioxins may act synergistically to prevent allergic diseases. Recently, Li et al. (36, 37) have reported the pharmacological actions of MSSM-002, a Chinese herbal formula used as an anti-asthma drug. The effects of MSSM-002 on animal models of allergy are similar to those observed for M50367, exhibiting IgE production inhibition and Th1-dominant differentiation with suppression of *GATA-3* expression. As MSSM-002 is a plant derivative that is abundant in a broad range of flavonoids, also probable AhR ligands, the antiallergic effects of this drug are likely mediated by AhR signaling.

We have demonstrated that M50367 is an AhR ligand of AhR that modulates the Th1/Th2 balance by influencing the differentiation of naive Th cells into Th1 dominance. This effect is probably mediated by down-regulation of *GATA-3* expression, resulting in antiallergic activity. These results suggest that AhR signaling plays a significant role in normal immune responses, making AhR signaling a promising target for chemo therapeutic agents for the treatment of allergic diseases.

Acknowledgments

We thank Yoshitaka Hosaka, Yusuke Shimizu and Tadashi Manabe for their helpful discussion.

Disclosures

The authors have no financial conflict of interest.

References

1. Denis, M., S. Cuthill, A. C. Wikstrom, L. Poellinger, and J. A. Gustafsson. 1988. Association of the dioxin receptor with the M_r 90,000 heat shock protein: a structural kinship with the glucocorticoid receptor. *Biochem. Biophys. Res. Commun.* 155: 801–807.
2. Perdew, G. H. 1988. Association of the Ah receptor with the 90-kDa heat shock protein. *J. Biol. Chem.* 263: 13802–13805.
3. Carver, L. A., J. J. LaPres, S. Jain, E. E. Dunham, and C. A. Bradfield. 1998. Characterization of the Ah receptor-associated protein, ARA9. *J. Biol. Chem.* 273: 33580–33587.
4. Kazlauskas, A., L. Poellinger, and I. Pongratz. 1999. Evidence that the co-chaperone p23 regulates ligand responsiveness of the dioxin (aryl hydrocarbon) receptor. *J. Biol. Chem.* 274: 13519–13524.
5. Fujii-Kuriyama, Y., M. Ema, J. Mimura, and K. Sogawa. 1994. Ah receptor: a novel ligand-activated transcription factor. *Exp. Clin. Immunogenet.* 1: 65–74.
6. Fernandez-Salguero, P. M., D. M. Hilbert, S. Rudikoff, J. M. Ward, and F. J. Gonzalez. 1996. Aryl-hydrocarbon receptor-deficient mice are resistant to 2,3,7,8-tetrachlorodibenzo-*p*-dioxin-induced toxicity. *Toxicol. Appl. Pharmacol.* 140: 173–179.
7. Silkworth, J. B., L. A. Antrim, and G. Sack. 1986. Ah receptor mediated suppression of the antibody response in mice is primarily dependent on the Ah phenotype of lymphoid tissue. *Toxicol. Appl. Pharmacol.* 86: 380–390.
8. Ohtake, F., K. Takeyama, T. Matsumoto, H. Kitagawa, Y. Yamamoto, K. Nohara, C. Tohyama, A. Krust, J. Mimura, P. Chambon, et al. 2003. Modulation of oestrogen receptor signaling by association with the activated dioxin receptor. *Nature* 423: 545–550.
9. Dragan, Y. P., and D. Schrenk. 2000. Animal studies addressing the carcinogenicity of TCDD (or related compounds) with an emphasis on tumour promotion. *Food Addit. Contam.* 17: 289–302.
10. Puga, A., C. R. Tomlinson, and Y. Xia. 2005. Ah receptor signals cross-talk with multiple developmental pathways. *Biochem. Pharmacol.* 69: 199–207.
11. Kerkvliet, N. I. 2002. Recent advances in understanding the mechanisms of TCDD immunotoxicity. *Int. Immunopharmacol.* 2: 277–291.
12. Kato, Y., T. Manabe, Y. Tanaka, and H. Mochizuki. 1999. Effect of an orally active Th1/Th2 balance modulator, M50367, on IgE production, eosinophilia, and airway hyper responsiveness in mice. *J. Immunol.* 162: 7470–7479.
13. Kato, Y., T. Negishi, S. Furusako, K. Mizuguchi, and H. Mochizuki. 2003. An orally active Th1/Th2 balance modulator, M50367, suppresses Th2 differentiation of naive Th cell in vitro. *Cell. Immunol.* 224: 29–37.
14. Fujisawa-Sehara, A., K. Sogawa, C. Nishi, and Y. Fujii-Kuriyama. 1986. Regulatory DNA elements localized remotely upstream from the drug-metabolizing cytochrome P-450c gene. *Nucleic Acids Res.* 14: 1465–1477.
15. McGuire, J., K. Okamoto, M. L. Whitelaw, H. Tanaka, and L. Poellinger. 2001. Definition of a dioxin receptor mutant that is a constitutive activator of transcription: delineation of overlapping repression and ligand binding functions within the PAS domain. *J. Biol. Chem.* 276: 41841–41849.
16. Ema, M., K. Sogawa, N. Watanabe, Y. Chujoh, N. Matsushita, O. Gotoh, Y. Funae, and Y. Fujii-Kuriyama. 1992. cDNA cloning and structure of mouse putative Ah receptor. *Biochem. Biophys. Res. Commun.* 184: 246–253.
17. Matsushita, N., K. Sogawa, M. Ema, A. Yoshida, and Y. Fujii-Kuriyama. 1993. A factor binding to the xenobiotic responsive element (XRE) of *P-450IA1* gene consists of at least two helix-loop-helix proteins, Ah receptor and Arnt. *J. Biol. Chem.* 268: 21002–21006.
18. Numayama-Tsuruta, K., A. Kobayashi, K. Sogawa, and Y. Fujii-Kuriyama. 1997. A point mutation responsible for defective function of the aryl-hydrocarbon-receptor nuclear translocator in mutant Hepa-1c1c7 cells. *Eur. J. Biochem.* 246: 486–495.
19. Zhou, J. G., E. C. Henry, C. M. Palermo, S. D. Dertinger, and T. A. Gasiewicz. 2003. Species-specific transcriptional activity of synthetic flavonoids in guinea pig and mouse cells as a result of differential activation of the aryl hydrocarbon receptor to interact with dioxin-responsive elements. *Mol. Pharmacol.* 63: 915–924.
20. Mimura, J., K. Yamashita, K. Nakamura, M. Morita, T. N. Takagi, K. Nakao, M. Ema, K. Sogawa, M. Yasuda, M. Katsuki, and Y. Fujii-Kuriyama. 1997. Loss of teratogenic response to 2,3,7,8-tetrachlorodibenzo-*p*-dioxin (TCDD) in mice lacking the Ah (dioxin) receptor. *Genes Cells* 2: 645–654.
21. Hirano, T., N. Yamakawa, H. Miyajima, K. Maeda, S. Takaki, A. Ueda, O. Taniguchi, H. Hashimoto, S. Hirose, K. Okumura, and Z. Ovary. 1989. An improved method for the detection of IgE Ab of defined specificity by ELISA using rat anti-IgE mAb. *J. Immunol. Methods* 119: 145–150.

22. Flynn, S., K. M. Toellner, C. Raykundalia, M. Goodall, and P. Lane. 1998. CD4 T cell cytokine differentiation: the B cell activation molecule, OX40 ligand, instructs CD4 T cells to express interleukin 4 and up-regulates expression of the chemokine receptor, Blr-1. *J. Exp. Med.* 188: 297–304
23. Assenmacher, M., M. Lohning, A. Scheffold, A. Richter, S. Miltenyi, J. Schmitz, and A. Radbruch. 1998. Commitment of individual Th1-like lymphocytes to expression of IFN-γ versus IL-4 and IL-10: selective induction of IL-10 by sequential stimulation of naive Th cells with IL-12 and IL-4. *J. Immunol.* 161: 2825–2832.
24. Miller, A. D., and F. Chen. 1996. 1996. Retrovirus packaging cells based on 10A1 murine leukemia virus for production of vectors that use multiple receptors for cell entry. *J. Virol.* 70: 5564–5571.
25. Casper, R. F., M. Quesne, I. M. Rogers, T. Shirota, A. Jolivet, E. Milgrom, and J. F. Savouret. 1999. Resveratrol has antagonist activity on the aryl hydrocarbon receptor: implications for prevention of dioxin toxicity. *Mol. Pharmacol.* 56: 784–790.
26. Zheng, W., and R. A. Flavell. 1997. The transcription factor GATA-3 is necessary and sufficient for Th2 cytokine gene expression in CD4 T cells. *Cell* 89: 587–596
27. Laiosa, M. D., A. Wyman, F. G. Murante, N. C. Fiore, J. E. Staples, T. A. Gasiewicz, and A. E. Silverstone. 2003. Cell proliferation arrest within intrathymic lymphocyte progenitor cells causes thymic atrophy mediated by the aryl hydrocarbon receptor. *J. Immunol.* 171: 4582–4591.
28. Fujimaki, H., K. Nohara, T. Kobayashi, K. Suzuki, K. Eguchi-Kasai, S. Tsukumo, M. Kijima, and C. Tohyama. 2002. Effect of a single oral dose of 2,3,7,8-tetrachlorodibenzo-*p*-dioxin on immune function in male NC/Nga mice. *Toxicol. Sci.* 66: 117–124.
29. Ito, T., K. Inouye, H. Fujimaki, C. Tohyama, and K. Nohara. 2002. Mechanism of TCDD-induced suppression of antibody production: effect on T cell-derived cytokine production in the primary immune reaction of mice. *Toxicol. Sci.* 70: 46–54.
30. Kerkvliet, N. I., D. M. Shepherd, and L. Baecher-Steppan. 2002. T lymphocytes are direct, aryl hydrocarbon receptor (AhR)-dependent targets of 2,3,7,8-tetrachlorodibenzo-*p*-dioxin (TCDD): AhR expression in both $CD4^+$ and $CD8^+$ T cells is necessary for full suppression of a cytotoxic T lymphocyte response by TCDD. *Toxicol. Appl. Pharmacol.* 185: 146–152.
31. Shepherd, D. M., E. A. Dearstyne, and N. I. Kerkvliet. 2000. The effects of TCDD on the activation of ovalbumin (OVA)-specific DO11.10 transgenic $CD4^+$ T cells in adoptively transferred mice. *Toxicol. Sci.* 56: 340–350.
32. George, K. M., M. W. Leonard, M. E. Roth, K. H. Lieuw, D. Kioussis, F. Grosveld, and J. D. Engel. 1994. Embryonic expression and cloning of the murine GATA-3 gene. *Development* 120: 2673–2686.
33. Fernandez-Salguero, P., T. Pineau, D. M. Hilbert, T. McPhail, S. S. Lee, S. Kimura, D. W. Nebert, S. Rudikoff, J. M. Ward, and F. J. Gonzalez. 1995. Immune system impairment and hepatic fibrosis in mice lacking the dioxin-binding Ah receptor. *Science* 268: 722–726.
34. Vorderstrasse, B. A., L. B. Steppan, A. E. Silverstone, and N. I. Kerkvliet. 2001. Aryl hydrocarbon receptor-deficient mice generate normal immune responses to model antigens and are resistant to TCDD-induced immune suppression. *Toxicol. Appl. Pharmacol.* 171: 157–164.
35. Weisglas-Kuperus, N., S. Patandin, G. A. Berbers, T. C. Sas, P. G. Mulder, P. J. Sauer, and H. Hooijkaas. 2000. Immunologic effects of background exposure to polychlorinated biphenyls and dioxins in Dutch preschool children. *Environ. Health Perspect.* 108: 1203–1207.
36. Li, X. M., C. K. Huang, T. F. Zhang, A. A. Teper, K. Srivastava, B. H. Schofield, and H. A. Sampson. 2000. The Chinese herbal medicine formula MSSM-002 suppresses allergic airway hyperreactivity and modulates Th1/Th2 responses in a murine model of allergic asthma. *J. Allergy Clin. Immunol.* 106: 660–668.
37. Srivastava, K., A. A. Teper, T. F. Zhang, S. Li, M. J. Walsh., C. K. Huang, M. Kattan, B. H. Schofield, H. A. Sampson, and X. M. Li. 2004. Immunomodulatory effect of the antiasthma Chinese herbal formula MSSM-002 on Th2 cells. *J. Allergy Clin. Immunol.* 113: 268–276.

MOLECULAR AND CELLULAR BIOLOGY, Nov. 2005, p. 10040–10051 Vol. 25, No. 22
0270-7306/05/$08.00+0 doi:10.1128/MCB.25.22.10040–10051.2005

Intrinsic Function of the Aryl Hydrocarbon (Dioxin) Receptor as a Key Factor in Female Reproduction

Takashi Baba,[1] Junsei Mimura,[2,4] Naohito Nakamura,[1,4] Nobuhiro Harada,[3] Masayuki Yamamoto,[2] Ken-ichirou Morohashi,[1,4]† and Yoshiaki Fujii-Kuriyama[2,4]*†

Department of Developmental Biology, National Institute for Basic Biology, 5-1 Higashiyama, Myodaiji-cho, Okazaki, Aichi 444-8787, Japan[1]; TARA Center, University of Tsukuba, 1-1-1 Tennoudai, Tsukuba, Ibaraki 305-8577, Japan[2]; Department of Biochemistry, Fujita Health University School of Medicine, 1-98 Dengakugakubo, Kutsukake-cho, Toyoake, Aichi 470-1192, Japan[3]; and Solution Oriented Research for Science and Technology, Japan Science and Technology Agency, 4-1-8 Honcho, Kawaguchi, Saitama 332-0012, Japan[4]

Received 20 May 2005/Returned for modification 2 July 2005/Accepted 3 September 2005

Dioxins exert a variety of adverse effects on organisms, including teratogenesis, immunosuppression, tumor promotion, and estrogenic action. Studies using aryl hydrocarbon receptor (AhR)-deficient mice suggest that the majority of these toxic effects are mediated by the AhR. In spite of the adverse effects mediated by this receptor, the AhR gene is conserved among a number of animal species, ranging from invertebrates to vertebrates. This high degree of conservation strongly suggests that AhR possesses an important physiologic function, and a critical function is also supported by the reduced fertility observed with AhR-null female mice. We demonstrate that AhR plays a crucial role in female reproduction by regulating the expression of ovarian P450 aromatase (*Cyp19*), a key enzyme in estrogen synthesis. As revealed by in vitro reporter gene assay and in vivo chromatin immunoprecipitation assay, AhR cooperates with an orphan nuclear receptor, Ad4BP/SF-1, to activate *Cyp19* gene transcription in ovarian granulosa cells. Administration to female mice of an AhR ligand, DMBA (9,10-dimethyl-1,2-benzanthracene), induced ovarian *Cyp19* gene expression, irrespective of the intrinsic phase of the estrus cycle. In addition to elucidating a physiological function for AhR, our studies also suggest a possible mechanism for the toxic effects of exogenous AhR ligands as endocrine disruptors.

The aryl hydrocarbon receptor (AhR), a member of the growing superfamily of basic helix-loop-helix (bHLH)-PAS transcription factors, functions as an intracellular mediator of xenobiotic signaling pathways (37). AhR was originally discovered to occur in hepatocytes as a transcription factor that binds with high affinity to an environmental contaminant, 2,3,7,8-tetrachlorodibenzo-*p*-dioxin (also referred to as TCDD or dioxin) (49). The molecular properties of AhR as a transcription factor have been elucidated by studies of *CYP1A1* gene expression. Normally, AhR exists in the cytoplasm as part of a complex with Hsp90, XAP2, and p23 (28, 34, 35). Upon binding of xenobiotics, such as TCDD and 3-methylcholanthrene (3MC), the receptor complex translocates into the nucleus, where AhR heterodimerizes with the AhR nuclear translocator (Arnt) (61). Within the nucleus, the AhR/Arnt heterodimer binds to XREs (*x*enobiotic *r*esponsive *e*lements) in the promoters of target genes to activate gene expression. A number of genes encoding drug-metabolizing enzymes, including *CYP1A1* and genes encoding UDP-glucuronosyl transferase and glutathione *S*-transferase, have been identified as targets of AhR (18, 21). Gene disruption studies have also revealed that AhR functions in the toxicological effects of dioxins, such as teratogenesis, immunosuppression, tumor promotion, and estrogenic action (6, 19, 38, 50, 56). Despite promoting these multiple adverse effects, AhR is conserved throughout a number of animal species, from invertebrates to vertebrates (20), suggesting that AhR plays a fundamental role in some physiologic process in addition to mediating the response to xenobiotics.

Ovarian functions are primarily regulated by the hypothalamus-pituitary-gonadal (HPG) axis. Gonadotropin-releasing hormone (GnRH) is discharged from the hypothalamic central nervous system and transported through the portal vascular system to stimulate the gonadotrophs of the anterior pituitary. Subsequently, the anterior pituitary secretes the gonadotropins follicle-stimulating hormone (FSH) and luteinizing hormone (LH) into the venous system. In the ovary, FSH promotes the development of immature follicles, eventually leading to the formation of mature preovulatory follicles. Upon stimulation with LH, the mature follicles rupture, leading to ovulation (52). Through the period of follicular maturation to ovulation, gonadotropins stimulate ovarian steroid synthesis. FSH upregulates expression of the P450 aromatase (*Cyp19*) gene (51), which catalyzes the final step of estrogenesis. Although the genes regulated by estradiol are largely unknown, the involvement of estradiol in folliculogenesis was revealed by the phenotype of *Cyp19* knockout (ArKO) mice (17). Due to impaired synthesis of estradiol, *Cyp19* knockout females displayed severely impaired follicular development, resulting in defective ovulation. Interestingly, ovarian defects similar to those seen with ArKO mice were observed upon simultaneous disruption of the estrogen receptor genes, ERα and ERβ (14).

* Corresponding author. Mailing address: TARA Center, University of Tsukuba, 1-1-1 Tennoudai, Tsukuba, Ibaraki 305-8577, Japan. Phone: 81-29-853-7323. Fax: 81-29-853-7318. E-mail: ykfujii@tara.tsukuba.ac.jp.

† These authors equally contributed to this work.

Our analysis of AhR-deficient mice revealed a phenotype defective in reproduction that was similar, albeit milder, to that seen with ArKO and ERα and ERβ double knockout (ERαβKO) mice. AhR-deficient female mice were subfertile, resulting from impaired folliculogenesis and ovulation. These ovarian defects were likely due to insufficient synthesis of estradiol, consistent with the observation that the *Cyp19* gene is a novel target gene of AhR within the ovary. While the mechanisms by which AhR induces drug-metabolizing enzyme genes in response to exogenous ligands have been extensively studied, the intrinsic function of AhR has remained unknown. In this report, we have identified an intrinsic function for AhR, in which this receptor adjusts ovarian estradiol concentrations by regulating *Cyp19* gene transcription. Based on this novel function for AhR, we propose a molecular mechanism by which the AhR ligands, such as DMBA (9,10-dimethyl-1,2-benzanthracene) and TCDD, also function as endocrine disruptors.

MATERIALS AND METHODS

Fertility assessment. For 3 months, eight $AhR^{+/+}$ and $AhR^{-/-}$ females each were mated with $AhR^{+/+}$ or $AhR^{+/-}$ males. The litter size of each pregnancy, average litter size, and total number of pups were determined. To exclude any effect caused by individual differences in male fertility, two female mice (one $AhR^{+/+}$ and one $AhR^{-/-}$) were housed in the same cage (mating cage) with a single male mouse ($AhR^{+/+}$ or $AhR^{+/-}$). Once known to be pregnant, female mice were isolated until they gave birth. The numbers of pups were counted on the day of bearing. Female mice were returned to mating cages the next day. This experiment continued for 3 months.

Determination of estrus cycle. To determine the estrus cycle phase, vaginal smears were collected by rinsing the vagina with phosphate-buffered saline (PBS) at 1700 h. Collected smears were mounted on glass slides and stained with Giemsa solution. When angular cells or nucleated epithelial cells occupied the majority of the smear, we determined that the mice were in proestrus or estrus. When a multitude of leukocytes were observed, animals were in metestrus or diestrus (42). These observations were performed for 21 consecutive days.

Superovulation. The estrus cycle was induced artificially by intraperitoneal injection of 5 U pregnant-mare serum gonadotropin (PMSG) (Teikoku Zouki, Japan) at 1700 h on day 1 of the experiment and 5 U human chorionic gonadotropin (hCG) (Teikoku Zouki, Japan) at 1700 h on day 3. In this superovulation protocol, follicles developed to the preovulatory stage following PMSG treatment, and ovulation was induced by hCG treatment. Experiments attempting to rescue $AhR^{-/-}$ ovulation required the intraperitoneal injection of β-estradiol (water soluble; Sigma) dissolved in PBS at 1700 h on day 2. Ovulated oocytes were collected from the oviduct and quantified on day 4.

Determination of serum LH concentrations. One hundred microliters of a GnRH agonist, buserelin (Sigma), in vehicle (PBS-0.3% bovine serum albumin) or vehicle alone was injected into the skin behind the necks of ovariectomized $AhR^{+/+}$ and $AhR^{-/-}$ females as described previously (11, 57). One hour after the injection, mice were anesthetized with diethyl ether. After collection of serum samples, serum LH concentrations were determined by radioimmunoassay (SRL, Inc., Japan).

Determination of hormone concentrations. After subjecting mice to the superovulation protocol, we collected ovaries at three time points during the preovulatory period (48 h after PMSG treatment [PMSG + 48 h], hCG + 5 h, and hCG + 8 h). Each ovary was weighed and then homogenized in diethyl ether to a concentration of 10 mg tissue/100 μl methanol. Aliquots (30 μl) of the redissolved materials were subjected to liquid chromatography-mass spectrometry (Applied Biotechnology, Inc., Japan) to determine the concentrations of estradiol and testosterone by comparing intensity values with standard curves made by standard hormones.

Immunohistochemistry. To detect LH, frozen sections (10 μm) were prepared from paraformaldehyde-fixed pituitaries of $AhR^{+/+}$ and $AhR^{-/-}$ mice, embedded in the Tissue-Tek compound (Sakura Finetechnical Co., Ltd., Japan). After being washed in Tris-buffered saline (50 mM Tris-HCl [pH 7.6], 150 mM NaCl) containing 1 mM $CaCl_2$, slides were boiled in 10 mM sodium citrate (pH 6.0) for antigen unmasking (43) and then treated with methanol at −20°C for 30 min. Sections were then incubated with an antibody against the β subunit of LH (Biogenesis) overnight at 4°C, washed, and treated with a biotinylated donkey anti-rabbit immunoglobulin G (Jackson ImmunoResearch Laboratories, Inc.) for 3 h at room temperature. After being washed, sections were developed with horseradish peroxidase-conjugated streptavidin (Nichirei, Japan) and visualized with diaminobenzidine (Nichirei, Japan) for 10 min at room temperature.

To detect AhR and Cyp19, we prepared paraffin sections (5 μm) from paraformaldehyde-fixed ovaries isolated from $AhR^{+/+}$ and $AhR^{-/-}$ females given PMSG and hCG (hCG + 5 h). After deparaffinization, sections were treated with proteinase K (20 μg/ml) (Sigma) to unmask antigen epitopes and then treated with hydrogen peroxide (0.3% H_2O_2 in methanol). Sections were incubated overnight at 4°C with either anti-AhR (generously provided by R. Pollenz) or anti-Cyp19 (22) antibody, washed, and then incubated with biotinylated donkey anti-rabbit immunoglobulin G for 3 h at room temperature. After being washed, sections were incubated with horseradish peroxidase-conjugated streptavidin and visualized with diaminobenzidine for 4 min at room temperature.

ChIP assay. We performed chromatin immunoprecipitation (ChIP) as previously described (46, 48), with the following modifications. Briefly, to fix the chromatin-protein complexes, ovaries isolated from $AhR^{+/+}$ and $AhR^{-/-}$ females treated with PMSG and hCG (hCG + 2 h) were punctured with a needle containing Dulbecco's modified Eagle's medium (DMEM)–Ham F-12 medium–1% FBS with 1% formaldehyde immediately after removal. After fixation was stopped in 125 mM glycine, the suspension of ovarian cells was filtered through a 70-μm cell strainer (Falcon). The isolated granulosa cells were then resuspended in lysis buffer (50 mM HEPES [pH 7.4], 140 mM NaCl, 1 mM EDTA, 10% glycerol, 0.5% NP-40, 0.25% Triton X-100). Nuclei were recovered by centrifugation at 4°C for 30 min. After dissolution in Tris-EDTA (10 mM Tris-HCl [pH 7.4], 0.1 mM EDTA), nuclei were sonicated to shear genomic DNA to approximately 1-kb fragments. Sheared chromatin-DNA complexes were then subjected to immunoprecipitation with either anti-AhR or anti-Ad4BP antibody (41). DNA was extracted from the precipitates by incubation with proteinase K at 65°C, followed by treatment with phenol-chloroform. Presence of the *Cyp19* promoter region was determined by PCR with the appropriate primer sets, indicated below.

Transfection and luciferase assay. The 5′-flanking regions of the human *CYP19* and mouse *Cyp19* genes were inserted into the pGL3-basic vector (Invitrogen) to generate h*CYP19*-3853Luc and m*Cyp19*-5335Luc, respectively. Human embryonic kidney-derived 293 cells were grown in DMEM (Sigma, St. Louis, Mo.) supplemented with 10% fetal bovine serum (FBS) at 37°C in 5% CO_2. Cells were plated at approximately 15% confluence 1 day before transfection. Transfections were conducted in triplicate in 24-well plates by using Lipofectamine Plus (Gibco BRL, Gaithersburg, Md.), according to the manufacturer's protocol. Each well received 500 ng reporter plasmid, 10 ng of the reference pBOS-LacZ vector, and one of various concentrations (0 to 50 ng) of the expression plasmid encoding either AhR, Arnt, the AhR repressor (AhRR) (36), or Ad4BP/SF-1 (39). Cells were treated for 3 h with lipofection reagent in DMEM without serum and then incubated for 48 h in DMEM-10% FBS with or without 3MC (Wako, Japan). Cells were harvested and subjected to luciferase and β-galactosidase assays. All luciferase activities were normalized to the corresponding β-galactosidase activities. Values are represented as the means ± standard deviations (SD) of three independent experiments.

Immunoprecipitation assay. The full-length cDNAs encoding AhR and Ad4BP/SF-1 were inserted into the expression vectors p3×FLAG-CMV-10 (Sigma) and pEGFP-c1 (Clontech) to generate 3×FLAG-AhR and EGFP-Ad4BP, respectively. These plasmids (1 μg) were cotransfected into 293 cells with the expression vector encoding Arnt as described above. An enhanced green fluorescent protein (EGFP) expression vector was included in the transfection as a control. Forty-six hours after transfection, 1 μM of 3MC was added to stimulate nuclear translocation of AhR. After a 2-h incubation, cells were harvested in lysis buffer (50 mM Tris-HCl [pH 8.0], 300 mM NaCl, 1.5 mM $MgCl_2$, 1 mM EDTA, 1% Triton X-100, 10% glycerol) containing 1× Complete protease inhibitor cocktail (Roche) (30). FLAG-tagged and associated proteins were immunoprecipitated from whole-cell extracts (400 μg) by using anti-FLAG M2-agarose affinity gel (Sigma) in immunoprecipitation buffer (50 mM Tris-HCl [pH 8.0], 150 mM NaCl, 1.5 mM $MgCl_2$, 1 mM EDTA, 1% Triton X-100, 10% glycerol) containing 1× Complete protease inhibitor cocktail. Isolated proteins were subjected to immunoblotting with an anti-GFP antibody (MBL, Nagoya, Japan).

PCR conditions. Primer pairs used for semiquantitative reverse transcription-PCR (RT-PCR) were as follows: AhR(fwd), 5′-CGC GGG CAC CAT GAG CAG-3′; AhR(rev), 5′-CTG TAA CAA GAA CTC TCC-3′; AhRR(fwd), 5′-GCT TTC TGT CCT GCG CCT C-3′; AhRR(rev), 5′-GAA GTC CTG CCG GTC ATC C-3′; Cyp19(fwd), 5′-TCA ATA CCA GGT CCT GGC TA-3′; Cyp19(rev), 5′-GTA TGC ACT GAT TCA CGT TC-3′; P450scc(fwd), 5′-CGA ATC GTC CTA AAC CAA GAG-3′; P450scc(rev), 5′-CAC TGA TGA CCC CTG AGA AAT-3′; 3β HSD(fwd), 5′-ACT GCA GGA GGT CAG AGC T-3′;

3β HSD(rev), 5′-GCC AGT AAC ACA CAG AAT ACC-3′; P450 17α(fwd), 5′-GGG GCA GGC ATA GAG ACA ACT-3′; P450 17α(rev), 5′-GGG TGT GGG TGT AAT GAG ATG-3′; $P27^{kip1}$(fwd), 5′-AAG CGG ATC ACC CCA AGC CT-3′; $P27^{kip1}$(rev), 5′-GTT GGC GGT TTT GTT TTG CG-3′; C/EBPβ(fwd), 5′-TCT ACT ACG AGC CCG ACT GCC T-3′; C/EBPβ(rev), 5′-AGCTTG TCC ACC GTC TTC TT-3′; GAPDH(fwd) (GAPDH, glyceraldehyde-3-phosphate dehydrogenase), 5′-GGC ATG GCC TTC CGT GTT CCT-3′; GAPDH(rev), TCC TTG CTG GGG TGG GTG GTC-3′; β-actin(fwd), 5′-ATG GAT GAC GAT ATC GCT-3′; and β-actin(rev), 5′-ATG AGG TAG TCT GTC AGG T-3′. Thermal-cycling conditions were as follows: 28 cycles of 30 s at 94°C, 30 s at 60°C, and 1 min at 72°C for the amplification of AhR, $P27^{kip1}$, and C/EBPβ; 32 cycles of 30 s at 94°C, 30 s at 58°C, and 1 min at 72°C for AhRR; 25 cycles of 30 s at 94°C, 30 s at 60°C, and 1 min at 72°C for Cyp19, P450scc, 3β HSD, and P450 17α; and 22 cycles of 30 s at 94°C, 30 s at 60°C, and 1 min at 72°C for GAPDH and β-actin. Quantitative RT-PCR was performed with a TaqMan gene expression assay (Applied Biosystems) on a 7500 real-time PCR system (Applied Biosystems). Thermal-cycling conditions were 50 cycles of 15 s at 95°C and 1 min at 60°C.

Primer pairs used for ChIP assays were as follows: XRE of Cyp19 (fwd), TGA GAG TGA ACT GCA GGA AG-3′; XRE of Cyp19 (rev), ACC TCA TGG CTA AGG CAA TG-3′; Ad4 of Cyp19 (fwd), ATA AGG AGG ATT GCC TCA GC-3′; Ad4 of Cyp19 (rev), GCT CCT GTC ACT TGG AAG GG-3′; −2740~−2441 of Cyp19 (fwd), GAC TTT GCA TAG AGA CTT GG-3′; −2740~−2441 of Cyp19 (rev), CTG TTT AGT GTT GTC AAT GC-3′; β-actin(fwd), AGG GTG TGA TGG TGG GAA TGG-3′; and β-actin(rev), TGG CTG GGG TGT TGA AGG TCT-3′. Thermal-cycling conditions were 32 cycles of 30 s at 94°C, 30 s at 62°C, and 1 min at 72°C.

RESULTS

Phenotype of $AhR^{-/-}$ females related to reproduction. The reproductive defects of $AhR^{-/-}$ females have remained controversial (1). We therefore examined if fertility was impaired in the $AhR^{-/-}$ females used in this study. To avoid experimental variation due to genetic background, we used AhR knockout (AhR KO) mice backcrossed to C57BL/6J mice for more than eight generations. For 3 months, $AhR^{+/+}$ and $AhR^{-/-}$ females were mated with $AhR^{+/+}$ or $AhR^{+/-}$ males, and the number of pups delivered was counted. Using eight randomly selected $AhR^{+/+}$ and $AhR^{-/-}$ females, the total number of pups delivered by the $AhR^{+/+}$ females was 213, while those delivered by $AhR^{-/-}$ females was 57 (Table 1). The average litter size of $AhR^{-/-}$ females was approximately 40% that of the wild type. None of the $AhR^{-/-}$ females examined bore a third litter, and one of these mutant animals was unable to deliver pups during the mating period. Although levels of reproductive activity varied among individuals, these results clearly indicated a decreased fertility of $AhR^{-/-}$ females.

To explore the causes of $AhR^{-/-}$ subfertility, we histologically examined the reproductive organs. Examination of the organs revealed a reduction of the ratio of ovarian weight to body weight in the $AhR^{-/-}$ females to 56% of that seen in the wild-type animals (0.055 ± 0.010% for $AhR^{+/+}$ versus 0.031 ± 0.003% for $AhR^{-/-}$, $n = 3$, $P < 0.05$). In contrast, the uterus appeared to be unaffected (0.272 ± 0.030% for $AhR^{+/+}$ versus 0.294 ± 0.049% for $AhR^{-/-}$, $n = 3$) (Fig. 1A and B). Based on histological analyses, the ovaries of $AhR^{-/-}$ animals developed follicles up to the antral/preovulatory stage in the presence of slightly hypoplastic interstitial cells (Fig. 1C). The corpus luteum, however, was barely detectable in $AhR^{-/-}$ ovaries. As the corpora lutea develop from postovulatory follicles, this observation implied a failure in a final step of follicular maturation and/or ovulation.

As failures of follicular maturation and ovulation are frequently accompanied by a disordered estrus cycle (29, 58), we then examined if the ovarian estrus cycle proceeds normally in $AhR^{-/-}$ mice (Fig. 1D). In wild-type and $AhR^{+/-}$ mice, the estrus cycle progressed regularly, lasting 4 to 5 days. Although we observed considerable individual variation, $AhR^{-/-}$ females displayed significantly disordered estrus cycles (Fig. 1D), which we classified into three groups. Mice in group I showed a prolonged cycle. In group II, animals exhibited a cycle that was irregularly shortened or prolonged. Unusually prolonged estrus phases were observed for mice classified as group III. Such irregularities were not observed for $AhR^{+/+}$ or $AhR^{+/-}$ mice.

As the HPG axis is crucial for progression of the estrus cycle, we examined the tissues of the HPG axis to determine which region is affected in $AhR^{-/-}$ animals. First, we examined the ability of the ovaries of $AhR^{-/-}$ mice to respond to gonadotropins. $AhR^{-/-}$ females aged 3 and 12 weeks were subjected to a standard superovulation protocol, and the numbers of ovulated oocytes in response to gonadotropin stimulation were counted. In $AhR^{-/-}$ mice, the total number of the ovulated oocytes decreased to approximately one-sixth the level seen for age-matched wild-type females (Table 2). We then examined the production of gonadotropins in the pituitaries of $AhR^{-/-}$ animals by immunohistochemical analysis using an anti-LH antibody (Fig. 2A). LH-immunoreactive gonadotrophs were present in the anterior lobes of the pituitary glands of both $AhR^{-/-}$ and $AhR^{+/+}$ mice. We then investigated the ability of gonadotrophs to secrete LH in response to stimulation with a GnRH agonist, buserelin (des-Gly_{10}-[D-Ser{t-Bu}$_6$]-LH-RH ethylamide). To exclude any feedback effects from the ovaries, animals were ovariectomized prior to experimentation. After subcutaneous injection of buserelin into the ovariectomized mice, we determined the serum LH concentrations. Neither the basal nor the buserelin-induced concentrations differed between $AhR^{+/+}$ and $AhR^{-/-}$ mice, indicating that the ability of $AhR^{-/-}$ gonadotrophs to se-

TABLE 1. Distribution of pups by female genotype

Genotype		No. of pups per litter				Total pups[b]
Female	Male	1st	2nd	3rd	Avg[a]	
$AhR^{+/+}$	$AhR^{+/-}$	8	11	10	9.7	29
		8	11		9.5	19
		10	10		10.0	20
		9	11	9	9.7	29
$AhR^{+/+}$	$AhR^{+/+}$	11	13	11	11.7	35
		9	10	11	10.0	30
		9	10	10	9.7	29
		11	11		11.0	22
$AhR^{-/-}$	$AhR^{+/-}$	4	5		4.5	9
		8			8.0	8
		3	5		4.0	8
						0
$AhR^{-/-}$	$AhR^{+/+}$	2	1		1.5	3
		2	3		2.5	5
		7	3		5.0	10
		10	4		7.0	14

[a] Average litter sizes for all $AhR^{+/+}$ females and $AhR^{-/-}$ females were 10.1 and 4.4, respectively.
[b] Total numbers of pups for all $AhR^{+/+}$ females and $AhR^{-/-}$ females were 213 and 57, respectively.

A

	total body (g)	ovary (mg)	ovary / body (%)	uterus (mg)	uterus / body (%)
AhR (+/+)	24.9	13.1 (5.6 + 7.5)	0.053	75.4	0.303
AhR (+/+)	23.1	10.6 (5.2 + 5.4)	0.046	56.3	0.244
AhR (+/+)	24.3	16.0 (8.2 + 7.8)	0.066	65.3	0.269
AhR (–/–)	22.0	7.1 (3.3 + 3.8)	0.032	72.9	0.331
AhR (–/–)	24.1	8.0 (3.2 + 4.8)	0.033	57.6	0.239
AhR (–/–)	21.5	5.8 (3.2 + 2.6)	0.027	67.2	0.313

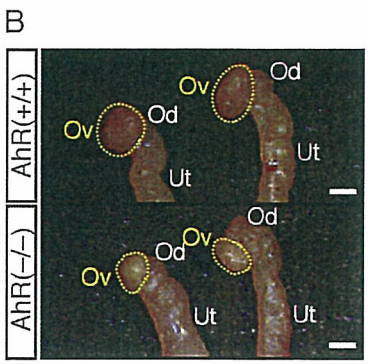

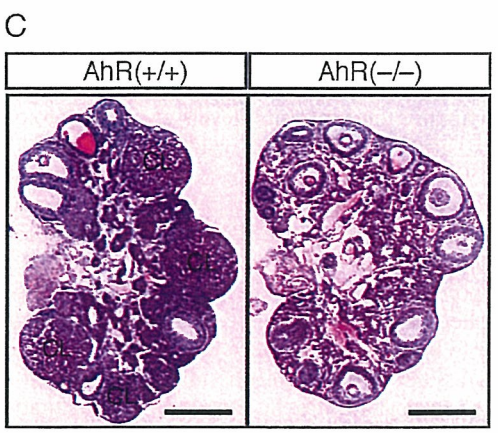

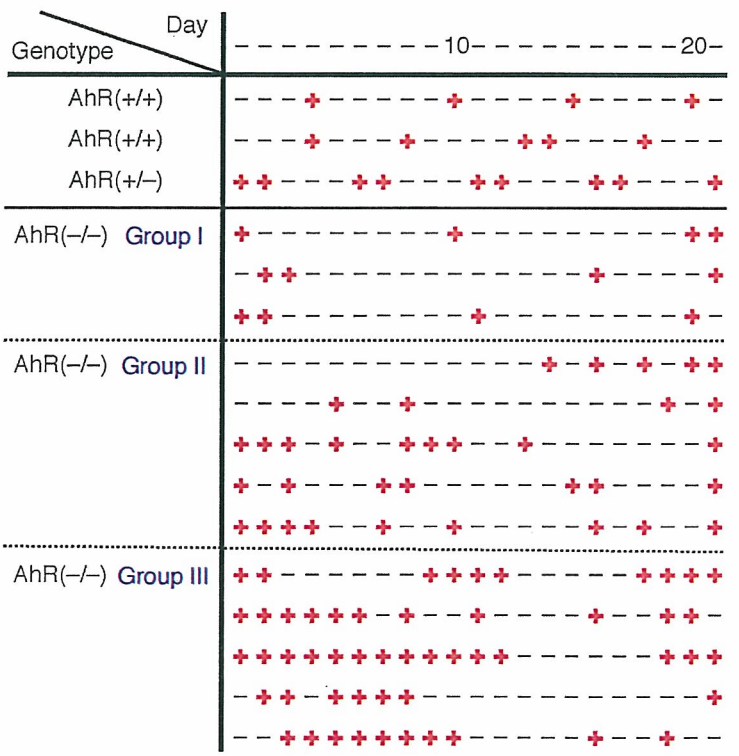

FIG. 1. Estrus cycle and folliculogenesis affected in $AhR^{-/-}$ ovaries. (A) Ovarian and uterine wet weights of $AhR^{+/+}$ and $AhR^{-/-}$ females. The ovaries and uteri isolated from 9-week-old mice were weighed. The ratios of ovarian or uterine wet weight to total body weight are also indicated. Three $AhR^{+/+}$ and $AhR^{-/-}$ mice each were examined in this experiment. (B) Morphologies of the reproductive tracts of 9-week-old $AhR^{+/+}$ and $AhR^{-/-}$ females. The ovaries are outlined in broken yellow lines. Ov, Od, and Ut indicate the ovary, oviduct, and uterus, respectively. Bar, 1 mm. (C) Histological analysis of the ovaries of $AhR^{+/+}$ and $AhR^{-/-}$ mice. Five-micrometer paraffin-embedded sections of $AhR^{+/+}$ and $AhR^{-/-}$ ovaries were stained with hematoxylin-eosin. CL indicates the corpus luteum. Bar, 0.5 mm. (D) Disordered estrus cycles in $AhR^{-/-}$ females. Vaginal smears from $AhR^{+/+}$, $AhR^{+/-}$, and $AhR^{-/-}$ female mice were collected for 21 consecutive days and stained with Giemsa solution. +, proestrus or estrus; –, metestrus or diestrus.

crete gonadotropins in response to upstream signals was not impaired (Fig. 2B). These results strongly suggest that the reduced fertility of $AhR^{-/-}$ females was due primarily to ovarian defects.

Synthesis of estradiol in $AhR^{-/-}$ ovaries is insufficient compared with that of the wild type. Estradiol is an essential sex hormone for female reproduction, and serum concentrations increase transiently during the preovulatory stage (54). We measured the concentrations of estradiol in the ovaries at three time points during the preovulatory stage (Fig. 3A). As $AhR^{-/-}$ females failed to demonstrate normal estrus cycles,

TABLE 2. Numbers of ovulated oocytes according to female genotype

Genotype	Age (wk)	No. of ovulated oocytes (mean ± SD)	No. of mice
$AhR^{+/+}$	3	51.3 ± 2.2	4
	12	25.0 ± 1.0	3
$AhR^{-/-}$	3	8.7 ± 8.5	3
	12	4.0 ± 4.6	3

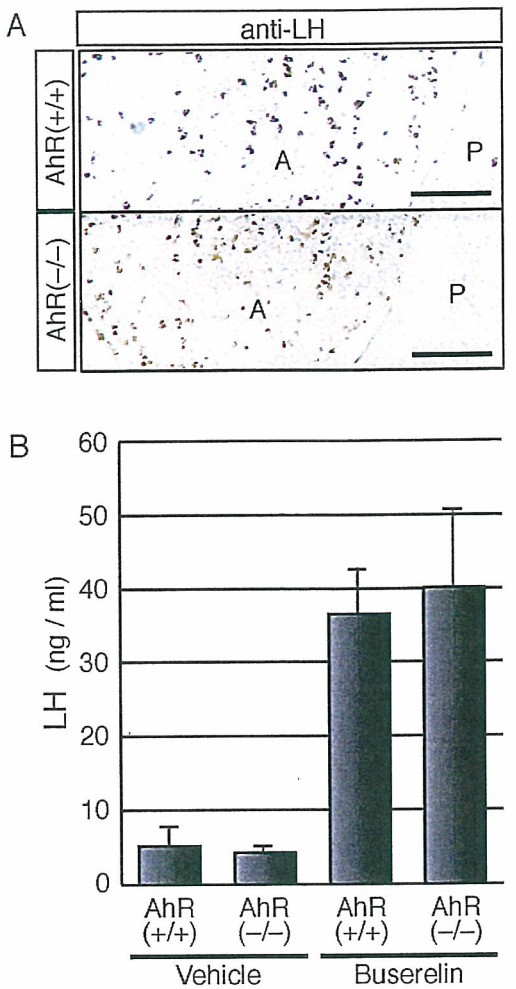

FIG. 2. Functionally normal gonadotropes of AhR$^{-/-}$ pituitaries. (A) Presence of gonadotrophs in the pituitary anterior lobes of AhR$^{-/-}$ females. Cryosections of pituitaries isolated from AhR$^{+/+}$ and AhR$^{-/-}$ mice were treated with an anti-LH antibody, which should specifically stain pituitary gonadotrophs. A and P represent the anterior and posterior lobes, respectively. Bar, 0.1 mm. (B) Secretion of LH from the gonadotrophs of AhR$^{-/-}$ pituitaries. A GnRH agonist, buserelin (2 μg), or vehicle alone was injected subcutaneously into ovariectomized AhR$^{+/+}$ and AhR$^{-/-}$ females. One hour after injection, serum levels of LH were determined. Values are represented as means ± SD for three to four mice.

we forced the estrus cycle to proceed by gonadotropin stimulation. In AhR$^{-/-}$ females, the concentrations of intraovary estradiol were decreased to 20 to 30% of the levels seen for wild-type animals at all three time points (Fig. 3B). Testosterone, the precursor of estradiol, was slightly increased in the ovaries of AhR$^{-/-}$ mice in comparison with the concentrations observed for AhR$^{+/+}$ females (Fig. 3C). These observations suggest that the decreases in ovarian estradiol are responsible for the reproductive defects of AhR$^{-/-}$ females. We therefore reasoned that an intraperitoneal injection of estradiol at the appropriate time of the ovulatory cycle would rescue the observed phenotype. AhR$^{-/-}$ mice were treated at day 2 with estradiol in the superovulation protocol (Fig. 3D), and then released oocytes were quantified. Administration of up to 10 ng estradiol to AhR$^{-/-}$ mice partially corrected the decrease in the number of ovulated oocytes in a dose-dependent manner. Administration of 20 ng estradiol failed to increase the number of ovulated oocytes further (Fig. 3E). Although these results clearly indicate that insufficient estradiol at least contributes to AhR$^{-/-}$ subfertility, either the timing or the site of estradiol administration may not have been optimal for full recovery of fertility. Additional factors may also be affected with AhR$^{-/-}$ mice, influencing the reproduction process.

AhR is indispensable for proper expression of the *Cyp19* gene in the ovary. As AhR functions as a transcription factor, the above observations suggested that this receptor is involved in the transcriptional regulation of steroidogenic genes. The expression pattern of AhR during folliculogenesis, however, is largely unknown. We therefore examined AhR expression throughout an artificially produced estrus cycle in wild-type mice (Fig. 4A). AhR mRNA was expressed throughout the preovulatory period. AhRR, a target of AhR transcriptional regulation, represses AhR function (2, 36). Interestingly, the expression of AhRR was upregulated at 6 and 7 h after hCG injection (Fig. 4B), suggesting that, while AhR becomes functionally active after treatment with PMSG, its activity thereafter is repressed by the action of AhRR. We therefore examined the expression of the *Cyp19* gene, whose product is essential for estradiol production, during folliculogenesis. *Cyp19* gene expression was activated 48 h after PMSG treatment and downregulated gradually after hCG treatment. This downregulation appeared to coincide with the induction of AhRR expression.

We then compared the expression levels of other steroidogenic enzymes within the ovaries of wild-type and AhR$^{-/-}$ mice at 4 and 7 h after hCG treatment (Fig. 4C). We did not observe any alteration in expression of mRNAs encoding steroidogenic Cyp11A (P450scc), 3β HSD, and Cyp17 (P450 17α, 17α-hydroxylase) between wild-type and knockout animals at the two time points examined. While Cyp19 mRNA was potently upregulated in wild-type ovaries during the final maturation stage of folliculogenesis induced by hormone treatment (Fig. 4B), expression of this gene was markedly reduced in AhR$^{-/-}$ ovaries, even at 4 h after hCG treatment. Quantitative RT-PCR demonstrated that the expression of Cyp19 in AhR$^{-/-}$ females was reduced by greater than 90% from that of wild-type animals 4 h after hCG treatment (Fig. 4D), indicating that Cyp19 mRNA expression was not upregulated in AhR$^{-/-}$ ovaries during hormone treatment. There were no detectable differences between the wild-type and AhR knockout mice in the expression of either p27^{kip1} or C/EBPβ, both of which are involved in ovulation (16, 29, 47, 58). As expected, there was no expression of AhRR mRNA in AhR$^{-/-}$ ovaries at 7 h after hCG treatment. To determine if Cyp19 protein levels were also altered in AhR$^{-/-}$ ovaries, we prepared whole-tissue extracts from hormone-treated ovaries (hCG + 5 h) and subjected these samples to Western blot analysis with an anti-Cyp19 antibody. In agreement with the results of our mRNA expression analysis, we detected decreased levels of Cyp19 protein in the ovaries of AhR$^{-/-}$ mice (Fig. 4E). Consistent with previous reports (53, 62), immunohistochemical staining with anti-AhR and anti-Cyp19 antibodies demonstrated coexpression of AhR and Cyp19 in the granulosa cells of antral follicles (Fig. 4F). We also confirmed by immunohis-

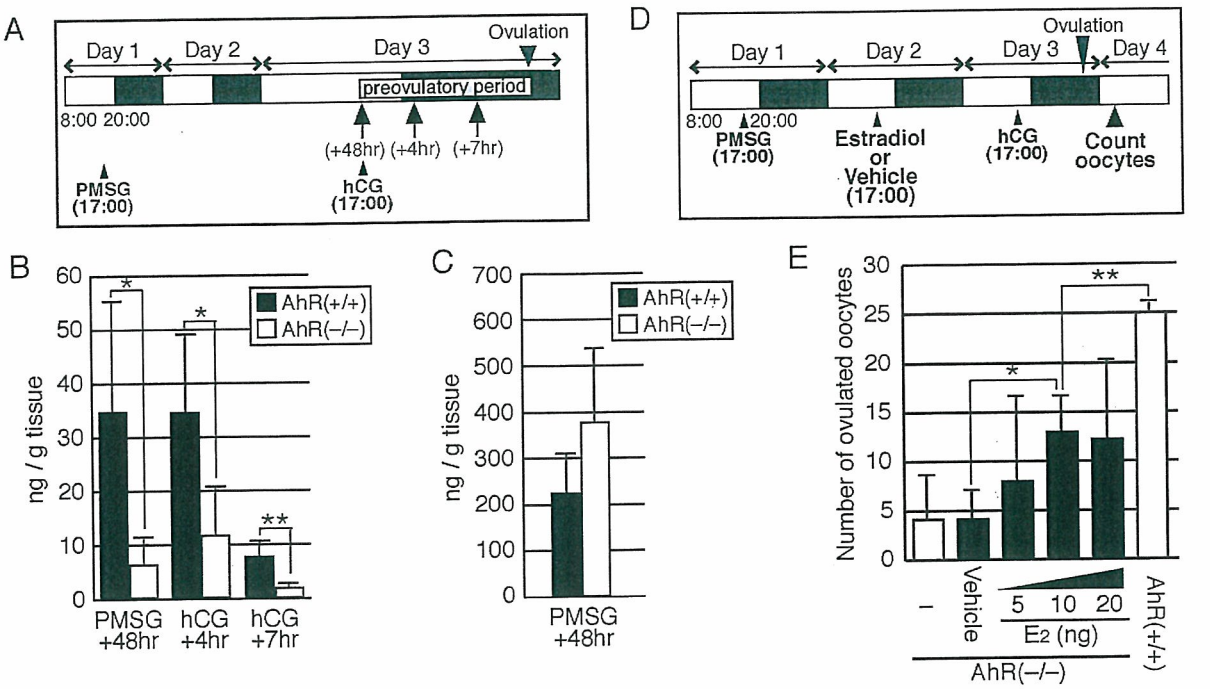

FIG. 3. Concentrations of intraovarian steroids in $AhR^{-/-}$ females and the rescue of ovulation by estradiol treatment. (A) Schematic representation of the experimental procedure used to determine intraovarian steroid concentrations during the preovulatory period. (B) Intraovarian estradiol concentrations in $AhR^{+/+}$ and $AhR^{-/-}$ females. The ovaries of at least three $AhR^{+/+}$ and three $AhR^{-/-}$ female mice were collected at the times indicated in panel A. Estradiol concentrations were then determined by liquid chromatography-mass spectrometry analysis. *, $P < 0.10$; **, $P < 0.05$. (C) Intraovarian testosterone concentrations were determined as described for panel B. (D) Schematic representation of the experimental estradiol administration procedure used to rescue the ovulation of $AhR^{-/-}$ mice. Mice treated with PMSG at day 1 were divided into two groups. One group was treated with various quantities of estradiol, while the other group was given vehicle alone on day 2. The mice from both groups were treated with hCG on day 3, and ovulation was assessed at day 4. (E) Effects of estradiol administration on ovulation in $AhR^{-/-}$ females. After the treatment of $AhR^{+/+}$ and $AhR^{-/-}$ females with PMSG and hCG, the oocytes released by ovulation were counted (open bars). $AhR^{-/-}$ females were also given an intraperitoneal injection of 5 to 20 ng 17β-estradiol (E2) or vehicle alone (filled bars) as described for panel D prior to counting the ovulated oocytes. *, $P < 0.025$; **, $P < 0.005$.

tochemistry that Cyp19 protein levels were diminished in the granulosa cells of $AhR^{-/-}$ ovaries (Fig. 4F).

AhR directly activates *Cyp19* gene transcription in cooperation with an orphan nuclear receptor, Ad4BP/SF-1. As the previously described results strongly suggest the involvement of AhR in *Cyp19* expression, we examined the mechanism by which AhR regulated *Cyp19* gene transcription. The *Cyp19* gene has multiple tissue-specific first exons (23, 33, 55). In the ovary, this gene is transcribed from exon PII (Ex 1d) in a mechanism involving the orphan nuclear receptor Ad4BP/SF-1 (8, 32, 40, 45). The binding site for Ad4BP/SF-1 is conserved within the 5′ upstream regions of the human and mouse genes. We also determined that the human *CYP19* and mouse *Cyp19* genes have an AhR/Arnt-binding sequence (XRE) 3,756 and 5,058 bp upstream of the ovary-specific first exon, respectively (Fig. 5A and B). We therefore transiently transfected the expression vectors of AhR, Arnt, and Ad4BP/SF-1 into cultured cells to investigate the promoter function of the *CYP19/Cyp19* genes. While Ad4BP/SF-1 clearly activated *CYP19/Cyp19* gene transcription, cotransfection of AhR and Arnt resulted in only weak activation. Simultaneous expression of AhR/Arnt with Ad4BP/SF-1, however, synergistically activated the Cyp19 promoter (Fig. 5C and D). Subsequent expression of AhRR suppressed the transcription activation induced by AhR (Fig. 5C and D).

The observed synergistic activation of the *CYP19/Cyp19* promoter by AhR/Arnt and Ad4BP/SF-1 implied a physical interaction between these proteins. To verify this interaction, we cotransfected expression vectors encoding 3×FLAG-AhR, Arnt, and EGFP-Ad4BP/SF-1 and then attempted to coimmunoprecipitate these components by using an anti-FLAG antibody. EGFP-Ad4BP/SF-1, but not EGFP, was coimmunoprecipitated with FLAG-AhR (Fig. 6A), indicating a potential physical interaction between AhR/Arnt and Ad4BP/SF-1. To investigate if AhR binds to the XRE within the promoter of *Cyp19* in vivo, we performed a ChIP assay using chromatin isolated from the granulosa cells of gonadotropin-treated ovaries (Fig. 6B). PCR analysis of the immunoprecipitates isolated using an anti-AhR antibody (Fig. 6B) revealed that the XRE of the *Cyp19* gene was associated with AhR in samples derived from wild-type mice but not $AhR^{-/-}$ mice (Fig. 6C). This result clearly indicates that AhR was recruited to the *Cyp19* promoter in vivo. As the *Cyp19* gene is synergistically activated by AhR/Arnt and Ad4BP/SF-1, we assumed that AhR, Arnt, and Ad4BP/SF-1 physically interact on the *Cyp19* promoter. We next examined whether anti-AhR antibodies precipitate

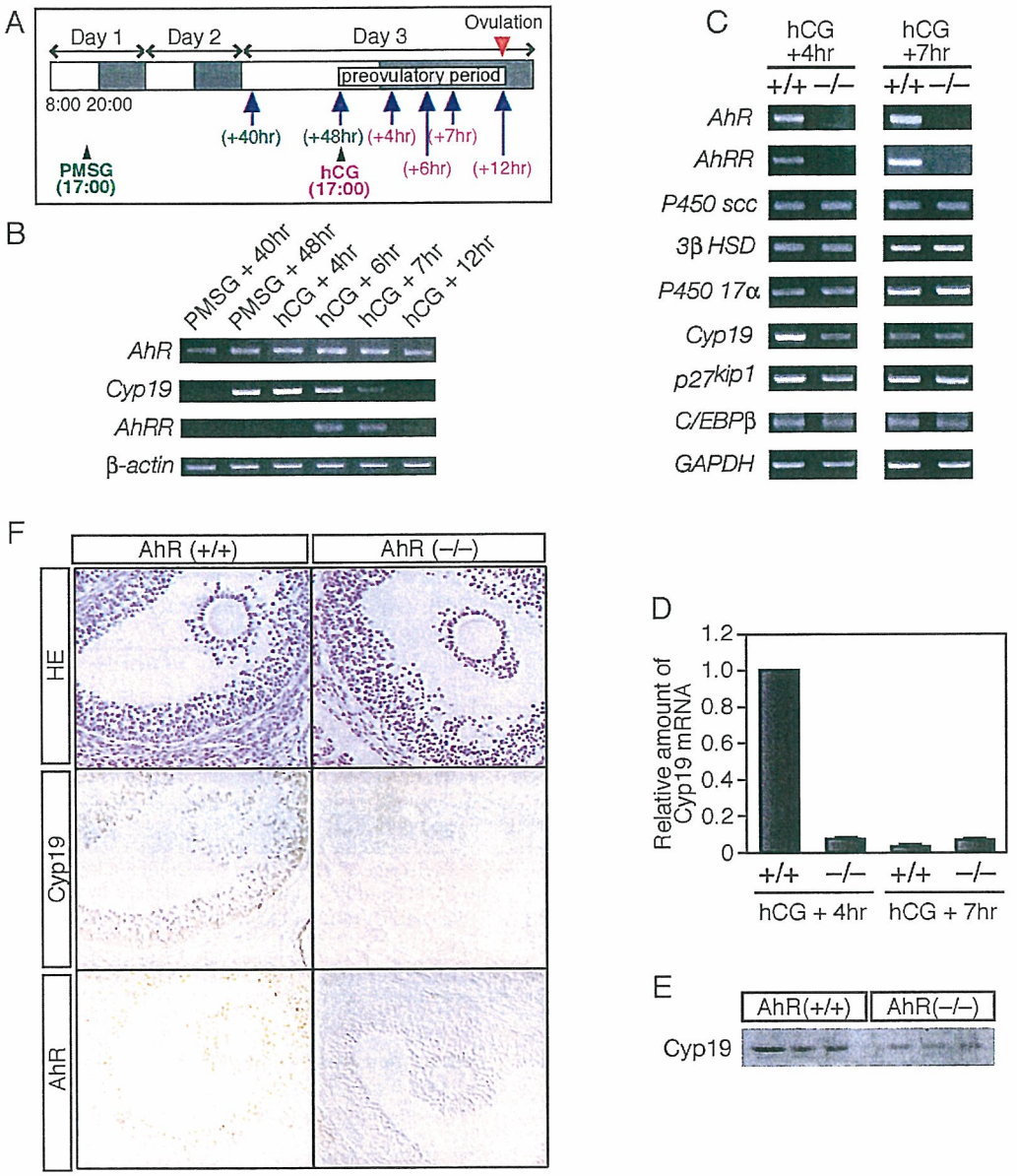

FIG. 4. AhR regulates the expression of ovarian *Cyp19* during the preovulatory period. (A) Schematic representation of the experimental procedure. The estrus cycle was induced artificially by intraperitoneal injection of PMSG at 1700 h on day 1 and of hCG at 1700 h on day 3. Ovaries were collected 40 and 48 h after PMSG injection or 4, 6, 7, and 12 h after hCG injection (indicated by arrows). (B) Profiles of mRNA expression for AhR, AhRR, and Cyp19 during the preovulatory period. Total RNA samples, prepared from ovaries derived from hormone-treated mice at the indicated times (top), were subjected to RT-PCR with primers sets specific for AhR, AhRR, and Cyp19. β-Actin mRNA was used as a control. (C) Expression of mRNAs encoding steroidogenic enzymes and proteins involved in ovarian folliculogenesis. Total RNA samples, prepared from the ovaries of hormone-treated $AhR^{+/+}$ and $AhR^{-/-}$ mice at the indicated times (top), were used for RT-PCR with the PCR primers. (D) Quantification of Cyp19 mRNA levels. Total RNA samples, prepared from the ovaries isolated 4 and 7 h after hCG injection, were subjected to quantitative RT-PCR analyses. Three animals were used for this experiment. (E) Expression of Cyp19 protein within $AhR^{+/+}$ and $AhR^{-/-}$ ovaries during the preovulatory period. Whole-cell extracts (10 μg), prepared from the ovaries of hormone-treated (hCG + 5 h) mice, were subjected to Western blot analysis with an anti-Cyp19 antibody. Three $AhR^{+/+}$ and three $AhR^{-/-}$ animals were used for these experiments. (F) Immunohistochemical staining of Cyp19 and AhR in the granulosa cells of $AhR^{+/+}$ and $AhR^{-/-}$ ovaries. Five-micrometer paraffin sections were prepared from the ovaries of hormone-treated (hCG + 5 h) mice. Sections were stained with hematoxylin-eosin (HE) or with anti-AhR or anti-Cyp19 antibody.

the Ad4 site of the *Cyp19* promoter and whether the anti-Ad4BP/SF-1 antibody reciprocally precipitates the XRE sequence. Both the XRE- and Ad4-containing sequences of the *Cyp19* promoter were recovered in both anti-Ad4BP/SF-1 and anti-AhR immunoprecipitates (Fig. 6D). As a control, the sequence between bp −2740 and −2441 was not recovered in either the anti-AhR or the anti-Ad4BP/SF-1 immunoprecipitate, excluding the possibility that incomplete fragmentation of

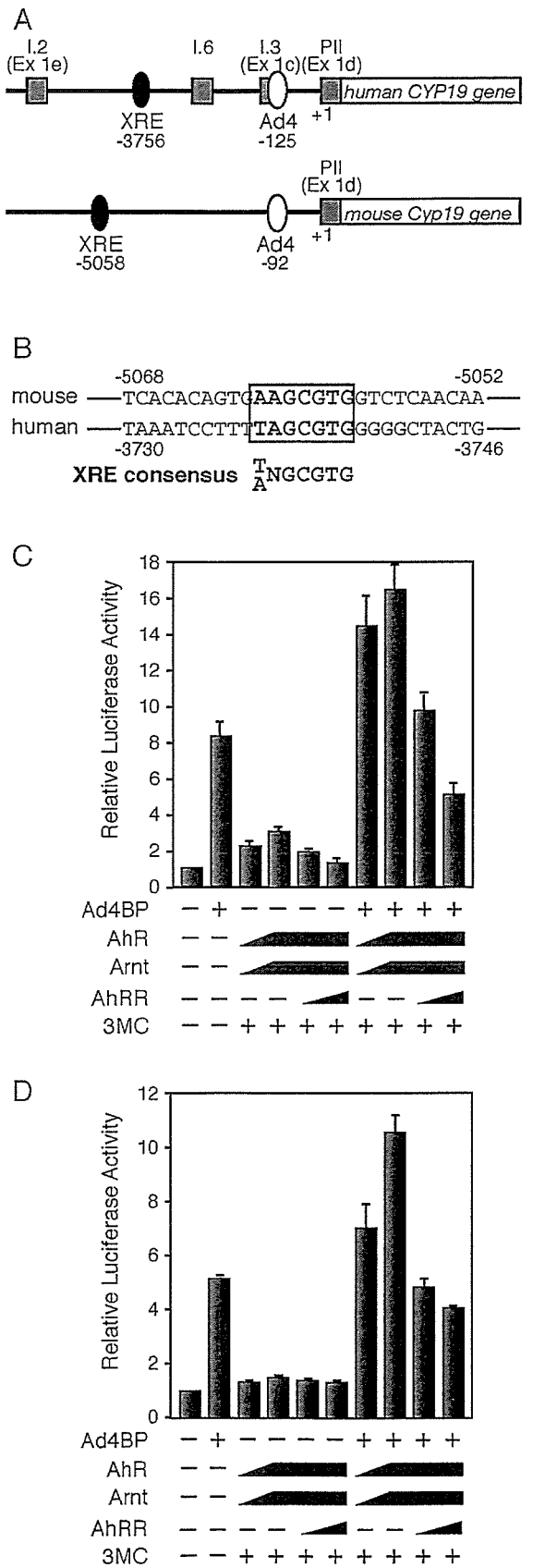

DNA during chromatin preparation resulted in artifactual coimmunoprecipitation of the Ad4- and XRE-containing sequences. To confirm the interaction between AhR and Ad4BP/SF-1 on the *Cyp19* promoter, we investigated whether the XRE is coimmunoprecipitated with Ad4BP/SF-1 in the $AhR^{-/-}$ chromatin (Fig. 6E). Anti-Ad4BP antibody failed to precipitate the XRE-containing sequence in the absence of AhR, indicating that Ad4BP/SF-1 does not bind directly to the XRE but binds indirectly through interaction with the XRE-bound AhR. In addition, we investigated whether AhR knockout affects Ad4BP/SF-1 binding to the Ad4 site and found that there is no difference in binding of Ad4BP/SF-1 between $AhR^{+/+}$ and $AhR^{-/-}$ mice (Fig. 6E). These results clearly demonstrated that both AhR and Ad4BP/SF-1 bind to their cognate binding sites within the *Cyp19* promoter and physically interact, probably leading to cooperative enhancement of *Cyp19* expression.

AhR ligands exerted an estrogenic effect by aberrantly activating *Cyp19* gene expression. While *Cyp19* is expressed transiently at a particular time point in the preovulatory period, AhR is constitutively expressed in granulosa cells. Inadvertently introduced AhR ligands may exert an estrogenic effect by aberrantly upregulating *Cyp19* expression in the ovary. To examine this possibility, we administered DMBA, an AhR ligand, to randomly selected female mice regardless of estrus cycle phase. After a 5-h treatment, we examined the expression of Cyp19 mRNA in the ovary. In a normal estrus cycle, expression of Cyp19 and the resultant estradiol production are induced transiently at proestrus. We observed that Cyp19 mRNA accumulated at proestrus but not at other phases of the estrus cycle in the ovaries of wild-type female mice (Fig. 7A and B). DMBA effectively induced *Cyp19* expression at most of the cycle phases except for metestrus. This reagent, however, failed to induce *Cyp19* gene expression in the ovaries of $AhR^{-/-}$ mice. Thus, AhR appears to have the potential to activate *Cyp19* gene transcription inappropriately in response to exogenous ligands, even when intrinsic estrogen synthesis should not be stimulated.

FIG. 5. Cooperative activation of AhR and Ad4BP/SF-1 on the *Cyp19/CYP19* promoter. (A) Schematic representation of the mouse *Cyp19* and human *CYP19* gene promoter regions. The square boxes indicate the first exons, exons I.2 (Ex 1e), I.6, I.3 (Ex 1c), and PII (Ex 1d), expressed specifically in the placenta, bone, adipose tissue, and ovary, respectively. The filled and open ovals represent the AhR/Arnt-binding (XRE) and Ad4BP/SF-1-binding (Ad4) sequences, respectively. The ovary-specific transcription start site is numbered as +1, and the positions of the XRE and Ad4 sites were numbered as the negative values of their distances from the transcription start site. (B) Nucleotide sequences containing the XRE site from the mouse *Cyp19* and human *CYP19* gene upstream regions. The consensus XRE sequence is indicated in bold letters. (C) Cooperative activation of AhR and Ad4BP/SF-1 on the human *CYP19* gene promoter. Expression plasmids encoding AhR, Arnt, AhRR, and Ad4BP/SF-1 were cotransfected into 293 cells with a reporter plasmid, in which luciferase expression is driven by the *CYP19* promoter (h*CYP19*-3853Luc), in the presence (+) or absence (−) of 3MC. After a 48-h incubation, cells were recovered and subjected to luciferase assays. All values are the means ± SD for three experiments. (D) Cooperative activation of AhR and Ad4BP/SF-1 on the mouse *Cyp19* promoter. m*Cyp19*-5335Luc was used for this assay. All other conditions were as specified for panel C.

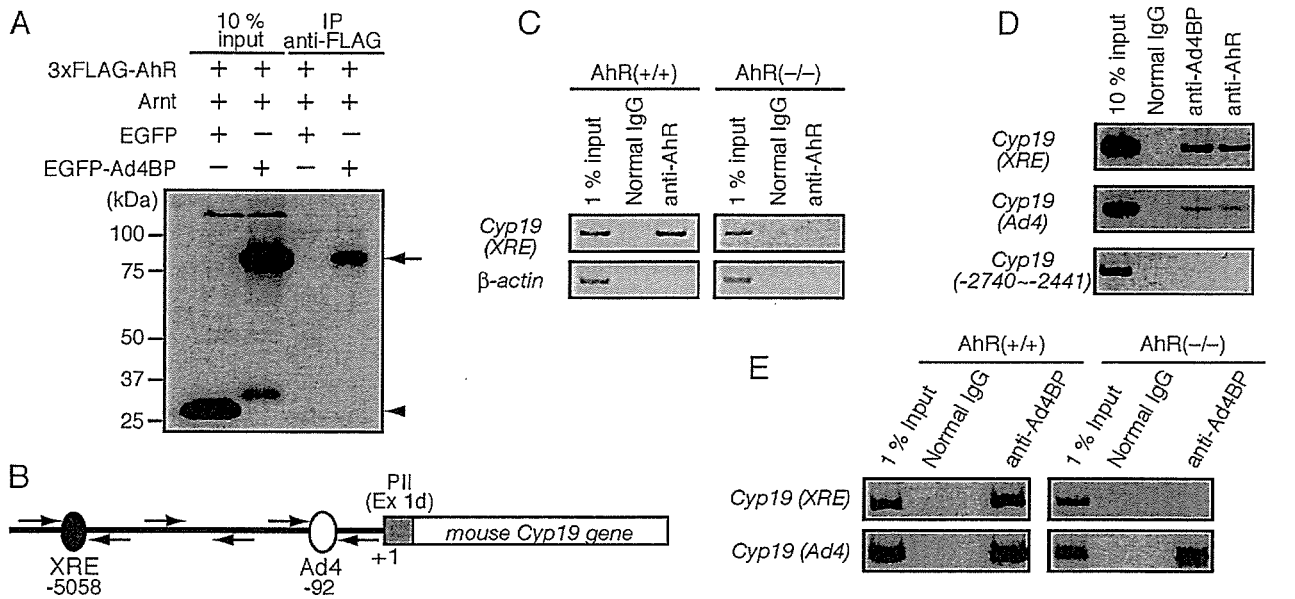

FIG. 6. Interaction of AhR with Ad4BP/SF-1 on the *Cyp19* promoter. (A) Detection of a physical interaction between AhR and Ad4BP/SF-1 by coimmunoprecipitation. FLAG-tagged proteins from whole-cell extracts of 293 cells transfected with 3×FLAG-AhR, Arnt, and EGFP-Ad4BP were immunoprecipitated (IP) with an anti-FLAG antibody. The immunoprecipitates were then subjected to immunoblotting with an anti-GFP antibody. An EGFP expression vector was transfected as a control. An arrow and an arrowhead indicate the EGFP-Ad4BP and EGFP samples, respectively. (B) Schematic representation of the location of primers used in the ChIP assays. Three sets of primers were used to amplify DNA regions containing the XRE site at −5058 and the Ad4/SF-1 sequence at −92 and a third unrelated region (−2740 to −2441), containing neither of them, as a control. (C) Binding of AhR to the promoter region of the *Cyp19* gene, revealed by ChIP assays. Soluble chromatin, prepared from preovulatory granulosa cells (hCG + 2 h), was subjected to ChIP assay with an anti-AhR antibody. β-Actin was used as a negative control. (D) Interaction between AhR and Ad4BP/SF-1 on the *Cyp19* gene promoter. Chromatin isolated from preovulatory granulosa cells was incubated with anti-AhR or anti-Ad4BP/SF-1 antibody and then subjected to PCR with two sets of primers amplifying the XRE and Ad4 sites. A primer pair specific for the sequence from −2740 to about −2441 was used as a control. (E) Binding of Ad4BP/SF-1 to the XRE and Ad4 sites in the presence or absence of AhR, revealed by ChIP assays. Chromatin isolated from preovulatory granulosa cells of the $AhR^{+/+}$ and $AhR^{-/-}$ ovaries was incubated with anti-Ad4BP/SF-1 or control antibody and then subjected to PCR to amplify the XRE and Ad4 sites. IgG, immunoglobulin G.

DISCUSSION

In agreement with a previous report (1), $AhR^{-/-}$ females demonstrated compromised fertility. The number of delivered pups was clearly decreased in comparison to those delivered by wild-type animals. As the phenotype of *AhR* gene disruption suggested a novel physiological function for AhR, in addition to its well-established xenobiotic metabolizing function, we investigated the molecular mechanisms underlying defective fertility in $AhR^{-/-}$ female mice.

Reproductive defects seen with $AhR^{-/-}$ female are primarily due to insufficient synthesis of estradiol in the ovary. Abbott et al. described that $AhR^{-/-}$ females exhibited difficulties in maintaining conceptuses during pregnancy (1), while Benedict et al. reported that AhR deficiency affected follicular maturation and ovulation under normal growth conditions (3, 4). Our studies indicated that follicles present in the ovaries of $AhR^{-/-}$ mice developed to an antral/preovulatory stage, while the corpus luteum was barely detectable. Upon stimulation of superovulation, the number of ovulated oocytes in $AhR^{-/-}$ females was significantly lower than those seen with the wild type. In conjunction with the observations of Benedict et al., these results suggested that the reduced fertility of $AhR^{-/-}$ females was a consequence of ovarian defects during the period of late folliculogenesis to follicular rupture.

Both implantation and follicular maturation are highly dependent on estrogenic action (12). The phenotype of $AhR^{-/-}$ mice suggested the hypothesis that the observed reproductive failure might be induced by the disruption of genes involved in estrogen production or action. The ovaries of ArKO mice were reported to contain many large follicles filled with granulosa cells, with an absence of a corpus luteum (17). ERαβKO female mice (14), completely lacking a receptor-mediated response to estrogen, failed to induce preovulatory follicle formation after superovulation treatment. The female reproduction defects of ArKO and ERαβKO mice resembled those of AhR KO mice, albeit with a more severe phenotype. The similarities between these phenotypes strongly suggested that AhR KO mice have deficits in estrogen production or action. After hypothesizing that estradiol production in the preovulatory period was affected in AhR KO females, we determined that intraovarian estrogen concentrations during the preovulatory stages were decreased in $AhR^{-/-}$ females. Administration of estradiol increased the number of ovulated oocytes in $AhR^{-/-}$ females, suggesting that the subfertility of $AhR^{-/-}$ mice results primarily from reduced levels of ovarian estrogen.

***Cyp19* gene transcription mediated synergistically by AhR and Ad4BP/SF-1.** Ovarian sex steroids, such as estrogen and progesterone, are synthesized from cholesterol through multi-

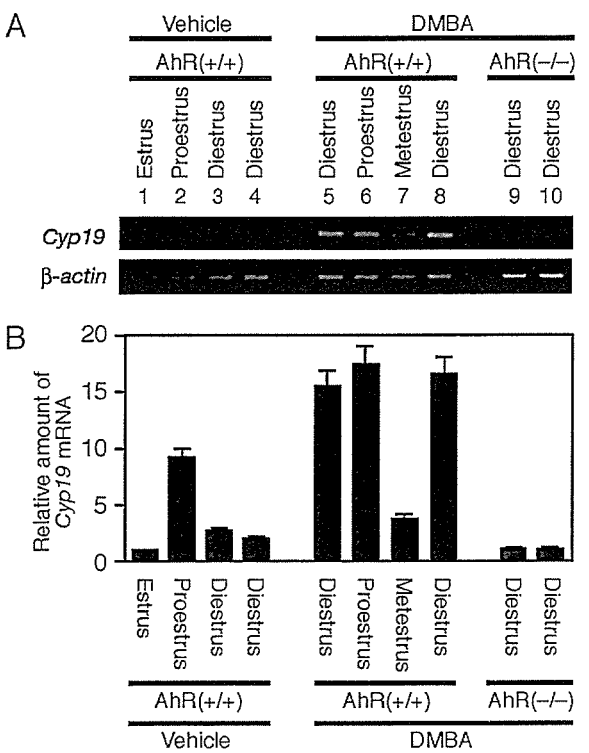

FIG. 7. Upregulation of *Cyp19* expression by an exogenous AhR ligand, DMBA. (A) Expression of *Cyp19* induced by intraperitoneal injection of DMBA. $AhR^{+/+}$ (lanes 1 to 8) or $AhR^{-/-}$ (lanes 9 and 10) female mice were injected intraperitoneally with DMBA (50 mg/kg of body weight) or vehicle alone. Five hours after injection, we prepared total RNA from the ovaries. The amounts of *Cyp19* mRNA were then evaluated by RT-PCR. The estrus cycle phase of each animal was determined by observing vaginal smears collected just before injection of DMBA. β-Actin was used as a control. (B) Quantitative representation of *Cyp19* mRNA levels. Quantification of the *Cyp19* transcript was performed by using a 7500 real-time PCR system (Applied Biosystems, Japan).

ple reactions in the ovary. Investigation of steroidogenic gene expression revealed that *Cyp19* expression was significantly reduced in $AhR^{-/-}$ females. Immunohistochemical and immunoblotting analyses confirmed the reduced levels of Cyp19 in granulosa cells. As Cyp19 is the rate-limiting enzyme in estrogen synthesis, it is likely that the reduced estradiol concentrations result primarily from lower levels of Cyp19 synthesis in the ovaries of $AhR^{-/-}$ females.

The *Cyp19* gene has multiple tissue-specific first exons (23, 33, 55). A survey of the 5′ sequence upstream of the ovary-specific first exon revealed the presence of a potential XRE sequence in both human and mouse genes. The presence of such an XRE sequence has recently been reported to occur within the promoter of the fish ovarian-type *CYP19* genes, although a functional analysis remains to be performed (7, 27, 59, 60). The conservation of XRE among a variety of animal species, however, suggests functionality of this sequence in the ovary-specific expression of *Cyp19*. In this study, we substantiated this hypothesis by transient transfection and ChIP assays. In addition, the *Cyp19* gene proximal promoter contained a functional Ad4/SF-1 site (32). Our investigation of the functional correlation between Ad4BP/SF-1 and AhR revealed that these factors cooperatively enhanced *Cyp19* gene transcription. This synergistic action resulted from a physical interaction, revealed by coimmunoprecipitation and ChIP assays.

Recently, another orphan nuclear receptor, LRH-1 (*l*iver *r*eceptor *h*omologue 1), has been reported to be selectively expressed in ovarian granulosa cells (15, 24) and to transactivate the ovary-specific *Cyp19* promoter in transient transfection assays. Structurally, LRH-1 exhibits homology with Ad4BP/SF-1, and the recognition sequences of these proteins are quite similar. Using the Ad4/SF-1 site from the *Cyp19* promoter as a probe, however, electrophoretic mobility shift assays revealed that Ad4BP/SF-1 is the dominant binding factor (9, 10, 15). These observations suggest that Ad4BP/SF-1 and LRH-1 play distinct roles in the regulation of target gene transcription. As LRH-1 is involved in cell proliferation via regulation of cyclin D1 and E1 gene expression (5), further investigations are needed to clarify the function of LRH-1 in the AhR-mediated expression of *Cyp19* in the ovary.

Role of negative feedback regulatory loop formed by AhR and AhRR. AhRR is one of the downstream targets of AhR transcriptional regulation (2, 36). Structurally, AhRR belongs to a family of bHLH-PAS transcription factors and suppresses AhR-mediated transactivation by competing with AhR for heterodimer formation with Arnt. This study confirmed the suppressive function of AhRR on *Cyp19* gene expression. The expressions of both AhRR and *Cyp19* are similarly regulated by AhR via binding of AhR to the XRE sequences in their promoters. Superovulation experiments, however, revealed that the *Cyp19* gene displayed an earlier peak of expression (reaching a maximum at 48 to 52 h after gonadotropin [PMSG] treatment) than AhRR, which was upregulated as *Cyp19* expression began to decline. Although the mechanisms producing this time lag of AhRR expression are unknown, cyclic expression of *Cyp19* in the estrus cycle could be explained by a lag in AhRR synthesis. From these observations, it is possible that AhR and AhRR regulate the ovarian biological clock governing the estrus cycle. In support of this possibility, it is interesting to note that expression of CLOCK and BMAL1 (Arnt3), two members of the bHLH-PAS family (to which AhR and AhRR belong), in the suprachiasmatic nuclei of the hypothalamus regulates the expression of their inhibitors, PERs, to generate the biological clock governing circadian rhythms (31).

In a normal ovarian cycle, the expression levels of AhR appear to be constant. Thus, to transactivate the expression of *Cyp19* and AhRR, AhR may also need to be activated. Although a number of endogenous ligands have been reported to activate AhR (13), the identity of the endogenous ligand required for the activation of AhR in the ovary and the mechanism by which this activation occurs during the estrus cycle remains unknown. In keratinocyte cell lines cultured at low density or in Ca^{2+}-free medium, AhR translocates to the nucleus to activate reporter genes, even in the absence of obvious AhR ligands (25). The activation of AhR by phosphorylation has been suggested for such cases (26).

Estrogenic effect of AhR ligand through two distinct mechanisms. In this study, we characterized the subfertility phenotype of $AhR^{-/-}$ female mice, identifying the key role of AhR in *Cyp19* gene transcription controlling the temporal synthesis

of ovarian estrogen in the estrus cycle. This intrinsic physiological role of AhR provides an explanation for the high degree of AhR conservation throughout vertebrate species. This finding also provides a molecular basis for the estrogenic actions of AhR ligands. DMBA, an AhR ligand, induced *Cyp19* expression, leading to unscheduled increases in estradiol regardless of estrus cycle phase. Recently, functional cross talk was reported between AhR and estrogen receptors (ER) (44), and the ligand-bound AhR exerts estrogenic effects through a direct interaction with nonliganded ER molecules associated with estrogen response elements in target gene promoters. Together with our observations, ligand-bound AhR likely exerts an estrogenic effect via two distinct mechanisms, the stimulation of estradiol production through the activation of *Cyp19* gene expression and the activation of empty ER by AhR coactivation.

ACKNOWLEDGMENTS

We thank R. S. Pollenz (University of South Florida) for kindly providing the AhR antibody and T. Etoh (Central Laboratories for Experimental Animals, Japan) for the care of laboratory mice. We are also grateful to Y. Nemoto for clerical work.

This work was funded in part by Core Research for Evolutionary Science and Technology, Solution Oriented Research for Science and Technology from Japan Science and Technology and Research Fellowship (T. Baba) of the Japan Society for the Promotion of Science for Young Scientists.

REFERENCES

1. **Abbott, B. D., J. E. Schmid, J. A. Pitt, A. R. Buckalew, C. R. Wood, G. A. Held, and J. J. Diliberto.** 1999. Adverse reproductive outcomes in the transgenic Ah receptor-deficient mouse. Toxicol. Appl. Pharmacol. **155:**62–70.
2. **Baba, T., J. Mimura, K. Gradin, A. Kuroiwa, T. Watanabe, Y. Matsuda, J. Inazawa, K. Sogawa, and Y. Fujii-Kuriyama.** 2001. Structure and expression of the Ah receptor repressor gene. J. Biol. Chem. **276:**33101–33110.
3. **Benedict, J. C., T. M. Lin, I. K. Loeffler, R. E. Peterson, and J. A. Flaws.** 2000. Physiological role of the aryl hydrocarbon receptor in mouse ovary development. Toxicol. Sci. **56:**382–388.
4. **Benedict, J. C., K. P. Miller, T. M. Lin, C. Greenfeld, J. K. Babus, R. E. Peterson, and J. A. Flaws.** 2003. Aryl hydrocarbon receptor regulates growth, but not atresia, of mouse preantral and antral follicles. Biol. Reprod. **68:** 1511–1517.
5. **Botrugno, O. A., E. Fayard, J. S. Annicotte, C. Haby, T. Brennan, O. Wendling, T. Tanaka, T. Kodama, W. Thomas, J. Auwerx, and K. Schoonjans.** 2004. Synergy between LRH-1 and beta-catenin induces G1 cyclin-mediated cell proliferation. Mol. Cell **15:**499–509.
6. **Brown, N. M., P. A. Manzolillo, J. X. Zhang, J. Wang, and C. A. Lamartiniere.** 1998. Prenatal TCDD and predisposition to mammary cancer in the rat. Carcinogenesis **19:**1623–1629.
7. **Callard, G. V., A. V. Tchoudakova, M. Kishida, and E. Wood.** 2001. Differential tissue distribution, developmental programming, estrogen regulation and promoter characteristics of *cyp19* genes in teleost fish. J. Steroid Biochem. Mol. Biol. **79:**305–314.
8. **Carlone, D. L., and J. S. Richards.** 1997. Functional interactions, phosphorylation, and levels of 3′,5′-cyclic adenosine monophosphate-regulatory element binding protein and steroidogenic factor-1 mediate hormone-regulated and constitutive expression of aromatase in gonadal cells. Mol. Endocrinol. **11:**292–304.
9. **Clyne, C. D., A. Kovacic, C. J. Speed, J. Zhou, V. Pezzi, and E. R. Simpson.** 2004. Regulation of aromatase expression by the nuclear receptor LRH-1 in adipose tissue. Mol. Cell. Endocrinol. **215:**39–44.
10. **Clyne, C. D., C. J. Speed, J. Zhou, and E. R. Simpson.** 2002. Liver receptor homologue-1 (LRH-1) regulates expression of aromatase in preadipocytes. J. Biol. Chem. **277:**20591–20597.
11. **Conn, P. M., J. G. Chafouleas, D. Rogers, and A. R. Means.** 1981. Gonadotropin releasing hormone stimulates calmodulin redistribution in rat pituitary. Nature **292:**264–265.
12. **Curtis Hewitt, S., E. H. Goulding, E. M. Eddy, and K. S. Korach.** 2002. Studies using the estrogen receptor alpha knockout uterus demonstrate that implantation but not decidualization-associated signaling is estrogen dependent. Biol. Reprod. **67:**1268–1277.
13. **Denison, M. S., and S. R. Nagy.** 2003. Activation of the aryl hydrocarbon receptor by structurally diverse exogenous and endogenous chemicals. Annu. Rev. Pharmacol. Toxicol. **43:**309–334.
14. **Dupont, S., A. Krust, A. Gansmuller, A. Dierich, P. Chambon, and M. Mark.** 2000. Effect of single and compound knockouts of estrogen receptors alpha (ERalpha) and beta (ERbeta) on mouse reproductive phenotypes. Development **127:**4277–4291.
15. **Falender, A. E., R. Lanz, D. Malenfant, L. Belanger, and J. S. Richards.** 2003. Differential expression of steroidogenic factor-1 and FTF/LRH-1 in the rodent ovary. Endocrinology **144:**3598–3610.
16. **Fero, M. L., M. Rivkin, M. Tasch, P. Porter, C. E. Carow, E. Firpo, K. Polyak, L. H. Tsai, V. Broudy, R. M. Perlmutter, K. Kaushansky, and J. M. Roberts.** 1996. A syndrome of multiorgan hyperplasia with features of gigantism, tumorigenesis, and female sterility in p27(Kip1)-deficient mice. Cell **85:**733–744.
17. **Fisher, C. R., K. H. Graves, A. F. Parlow, and E. R. Simpson.** 1998. Characterization of mice deficient in aromatase (ArKO) because of targeted disruption of the *cyp19* gene. Proc. Natl. Acad. Sci. USA **95:**6965–6970.
18. **Fujisawa-Sehara, A., K. Sogawa, M. Yamane, and Y. Fujii-Kuriyama.** 1987. Characterization of xenobiotic responsive elements upstream from the drug-metabolizing cytochrome P-450c gene: a similarity to glucocorticoid regulatory elements. Nucleic Acids Res. **15:**4179–4191.
19. **Gibbons, A.** 1993. Dioxin tied to endometriosis. Science **262:**1373.
20. **Hahn, M. E.** 2002. Aryl hydrocarbon receptors: diversity and evolution. Chem.-Biol. Interact. **141:**131–160.
21. **Hankinson, O.** 1995. The aryl hydrocarbon receptor complex. Annu. Rev. Pharmacol. Toxicol. **35:**307–340.
22. **Harada, N.** 1988. Novel properties of human placental aromatase as cytochrome P-450: purification and characterization of a unique form of aromatase. J. Biochem. (Tokyo) **103:**106–113.
23. **Harada, N., T. Utsumi, and Y. Takagi.** 1993. Tissue-specific expression of the human aromatase cytochrome P-450 gene by alternative use of multiple exons 1 and promoters, and switching of tissue-specific exons 1 in carcinogenesis. Proc. Natl. Acad. Sci. USA **90:**11312–11316.
24. **Hinshelwood, M. M., J. J. Repa, J. M. Shelton, J. A. Richardson, D. J. Mangelsdorf, and C. R. Mendelson.** 2003. Expression of LRH-1 and SF-1 in the mouse ovary: localization in different cell types correlates with differing function. Mol. Cell. Endocrinol. **207:**39–45.
25. **Ikuta, T., Y. Kobayashi, and K. Kawajiri.** 2004. Cell density regulates intracellular localization of aryl hydrocarbon receptor. J. Biol. Chem. **279:** 19209–19216.
26. **Ikuta, T., Y. Kobayashi, and K. Kawajiri.** 2004. Phosphorylation of nuclear localization signal inhibits the ligand-dependent nuclear import of aryl hydrocarbon receptor. Biochem. Biophys. Res. Commun. **317:**545–550.
27. **Kazeto, Y., S. Ijiri, A. R. Place, Y. Zohar, and J. M. Trant.** 2001. The 5′-flanking regions of CYP19A1 and CYP19A2 in zebrafish. Biochem. Biophys. Res. Commun. **288:**503–508.
28. **Kazlauskas, A., L. Poellinger, and I. Pongratz.** 1999. Evidence that the co-chaperone p23 regulates ligand responsiveness of the dioxin (aryl hydrocarbon) receptor. J. Biol. Chem. **274:**13519–13524.
29. **Kiyokawa, H., R. D. Kineman, K. O. Manova-Todorova, V. C. Soares, E. S. Hoffman, M. Ono, D. Khanam, A. C. Hayday, L. A. Frohman, and A. Koff.** 1996. Enhanced growth of mice lacking the cyclin-dependent kinase inhibitor function of p27(Kip1). Cell **85:**721–732.
30. **Komatsu, T., H. Mizusaki, T. Mukai, H. Ogawa, D. Baba, M. Shirakawa, S. Hatakeyama, K. I. Nakayama, H. Yamamoto, A. Kikuchi, and K. Morohashi.** 2004. Small ubiquitin-like modifier 1 (SUMO-1) modification of the synergy control motif of Ad4 binding protein/steroidogenic factor 1 (Ad4BP/SF-1) regulates synergistic transcription between Ad4BP/SF-1 and Sox9. Mol. Endocrinol. **18:**2451–2462.
31. **Lowrey, P. L., and J. S. Takahashi.** 2000. Genetics of the mammalian circadian system: photic entrainment, circadian pacemaker mechanisms, and posttranslational regulation. Annu. Rev. Genet. **34:**533–562.
32. **Lynch, J. P., D. S. Lala, J. J. Peluso, W. Luo, K. L. Parker, and B. A. White.** 1993. Steroidogenic factor 1, an orphan nuclear receptor, regulates the expression of the rat aromatase gene in gonadal tissues. Mol. Endocrinol. **7:**776–786.
33. **Means, G. D., M. W. Kilgore, M. S. Mahendroo, C. R. Mendelson, and E. R. Simpson.** 1991. Tissue-specific promoters regulate aromatase cytochrome P450 gene expression in human ovary and fetal tissues. Mol. Endocrinol. **5:**2005–2013.
34. **Meyer, B. K., and G. H. Perdew.** 1999. Characterization of the AhR-hsp90-XAP2 core complex and the role of the immunophilin-related protein XAP2 in AhR stabilization. Biochemistry **38:**8907–8917.
35. **Meyer, B. K., M. G. Pray-Grant, J. P. Vanden Heuvel, and G. H. Perdew.** 1998. Hepatitis B virus X-associated protein 2 is a subunit of the unliganded aryl hydrocarbon receptor core complex and exhibits transcriptional enhancer activity. Mol. Cell. Biol. **18:**978–988.
36. **Mimura, J., M. Ema, K. Sogawa, and Y. Fujii-Kuriyama.** 1999. Identification of a novel mechanism of regulation of Ah (dioxin) receptor function. Genes Dev. **13:**20–25.
37. **Mimura, J., and Y. Fujii-Kuriyama.** 2003. Functional role of AhR in the expression of toxic effects by TCDD. Biochim. Biophys. Acta **1619:**263–268.
38. **Mimura, J., K. Yamashita, K. Nakamura, M. Morita, T. N. Takagi, K. Nakao, M. Ema, K. Sogawa, M. Yasuda, M. Katsuki, and Y. Fujii-Kuriyama.**

1997. Loss of teratogenic response to 2,3,7,8-tetrachlorodibenzo-*p*-dioxin (TCDD) in mice lacking the Ah (dioxin) receptor. Genes Cells **2:**645–654.

39. **Mizusaki, H., K. Kawabe, T. Mukai, E. Ariyoshi, M. Kasahara, H. Yoshioka, A. Swain, and K. Morohashi.** 2003. *Dax-1* (dosage-sensitive sex reversal-adrenal hypoplasia congenita critical region on the X chromosome, gene 1) gene transcription is regulated by Wnt4 in the female developing gonad. Mol. Endocrinol. **17:**507–519.
40. **Morohashi, K., S. Honda, Y. Inomata, H. Handa, and T. Omura.** 1992. A common trans-acting factor, Ad4-binding protein, to the promoters of steroidogenic P-450s. J. Biol. Chem. **267:**17913–17919.
41. **Morohashi, K., U. M. Zanger, S. Honda, M. Hara, M. R. Waterman, and T. Omura.** 1993. Activation of CYP11A and CYP11B gene promoters by the steroidogenic cell-specific transcription factor, Ad4BP. Mol. Endocrinol. **7:**1196–1204.
42. **Nelson, J. F., L. S. Felicio, P. K. Randall, C. Sims, and C. E. Finch.** 1982. A longitudinal study of estrous cyclicity in aging C57BL/6J mice. I. Cycle frequency, length and vaginal cytology. Biol. Reprod. **27:**327–339.
43. **Nomura, M., K. Kawabe, S. Matsushita, S. Oka, O. Hatano, N. Harada, H. Nawata, and K. Morohashi.** 1998. Adrenocortical and gonadal expression of the mammalian Ftz-F1 gene encoding Ad4BP/SF-1 is independent of pituitary control. J. Biochem. (Tokyo) **124:**217–224.
44. **Ohtake, F., K. Takeyama, T. Matsumoto, H. Kitagawa, Y. Yamamoto, K. Nohara, C. Tohyama, A. Krust, J. Mimura, P. Chambon, J. Yanagisawa, Y. Fujii-Kuriyama, and S. Kato.** 2003. Modulation of oestrogen receptor signalling by association with the activated dioxin receptor. Nature **423:** 545–550.
45. **Omura, T., and K. Morohashi.** 1995. Gene regulation of steroidogenesis. J. Steroid Biochem. Mol. Biol. **53:**19–25.
46. **Orlando, V., H. Strutt, and R. Paro.** 1997. Analysis of chromatin structure by in vivo formaldehyde cross-linking. Methods **11:**205–214.
47. **Pall, M., P. Hellberg, M. Brannstrom, M. Mikuni, C. M. Peterson, K. Sundfeldt, B. Norden, L. Hedin, and S. Enerback.** 1997. The transcription factor C/EBP-beta and its role in ovarian function; evidence for direct involvement in the ovulatory process. EMBO J. **16:**5273–5279.
48. **Parekh, B. S., and T. Maniatis.** 1999. Virus infection leads to localized hyperacetylation of histones H3 and H4 at the IFN-beta promoter. Mol. Cell **3:**125–129.
49. **Poland, A., E. Glover, and A. S. Kende.** 1976. Stereospecific, high affinity binding of 2,3,7,8-tetrachlorodibenzo-*p*-dioxin by hepatic cytosol. Evidence that the binding species is receptor for induction of aryl hydrocarbon hydroxylase. J. Biol. Chem. **251:**4936–4946.
50. **Poland, A., and J. C. Knutson.** 1982. 2,3,7,8-tetrachlorodibenzo-*p*-dioxin and related halogenated aromatic hydrocarbons: examination of the mechanism of toxicity. Annu. Rev. Pharmacol. Toxicol. **22:**517–554.
51. **Richards, J. S.** 1994. Hormonal control of gene expression in the ovary. Endocr. Rev. **15:**725–751.
52. **Richards, J. S.** 2001. Perspective: the ovarian follicle—a perspective in 2001. Endocrinology **142:**2184–2193.
53. **Robles, R., Y. Morita, K. K. Mann, G. I. Perez, S. Yang, T. Matikainen, D. H. Sherr, and J. L. Tilly.** 2000. The aryl hydrocarbon receptor, a basic helix-loop-helix transcription factor of the PAS gene family, is required for normal ovarian germ cell dynamics in the mouse. Endocrinology **141:**450–453.
54. **Roby, K. F.** 2001. Alterations in follicle development, steroidogenesis, and gonadotropin receptor binding in a model of ovulatory blockade. Endocrinology **142:**2328–2335.
55. **Sebastian, S., and S. E. Bulun.** 2001. A highly complex organization of the regulatory region of the human CYP19 (aromatase) gene revealed by the Human Genome Project. J. Clin. Endocrinol. Metab. **86:**4600–4602.
56. **Shimizu, Y., Y. Nakatsuru, M. Ichinose, Y. Takahashi, H. Kume, J. Mimura, Y. Fujii-Kuriyama, and T. Ishikawa.** 2000. Benzo[*a*]pyrene carcinogenicity is lost in mice lacking the aryl hydrocarbon receptor. Proc. Natl. Acad. Sci. USA **97:**779–782.
57. **Stanislaus, D., J. A. Janovick, T. Ji, T. M. Wilkie, S. Offermanns, and P. M. Conn.** 1998. Gonadotropin and gonadal steroid release in response to a gonadotropin-releasing hormone agonist in Gqalpha and G11alpha knockout mice. Endocrinology **139:**2710–2717.
58. **Sterneck, E., L. Tessarollo, and P. F. Johnson.** 1997. An essential role for C/EBPbeta in female reproduction. Genes Dev. **11:**2153–2162.
59. **Tchoudakova, A., M. Kishida, E. Wood, and G. V. Callard.** 2001. Promoter characteristics of two *cyp19* genes differentially expressed in the brain and ovary of teleost fish. J. Steroid Biochem. Mol. Biol. **78:**427–439.
60. **Tong, S. K., and B. C. Chung.** 2003. Analysis of zebrafish *cyp19* promoters. J. Steroid Biochem. Mol. Biol. **86:**381–386.
61. **Whitelaw, M., I. Pongratz, A. Wilhelmsson, J.-Å. Gustafsson, and L. Poellinger.** 1993. Ligand-dependent recruitment of the Arnt coregulator determines DNA recognition by the dioxin receptor. Mol. Cell. Biol. **13:** 2504–2514.
62. **Yoshinaga-Hirabayashi, T., K. Ishimura, H. Fujita, J. Kitawaki, and Y. Osawa.** 1990. Immunocytochemical localization of aromatase in immature rat ovaries treated with PMSG and hCG, and in pregnant rat ovaries. Histochemistry **93:**223–228.

MOLECULAR AND CELLULAR BIOLOGY, Nov. 2005, p. 9360–9368 Vol. 25, No. 21
0270-7306/05/$08.00+0 doi:10.1128/MCB.25.21.9360–9368.2005

Constitutive Expression of Aryl Hydrocarbon Receptor in Keratinocytes Causes Inflammatory Skin Lesions

Masafumi Tauchi,[1,2] Azumi Hida,[1,2] Takaaki Negishi,[3] Fumiki Katsuoka,[1,2] Shuhei Noda,[1,2] Junsei Mimura,[1,2,6] Tomonori Hosoya,[4] Akinori Yanaka,[1] Hiroyuki Aburatani,[5] Yoshiaki Fujii-Kuriyama,[2,6] Hozumi Motohashi,[1,2]* and Masayuki Yamamoto[1,2,4]

Graduate School of Comprehensive Human Sciences[1] and Center for Tsukuba Advanced Research Alliance,[2] University of Tsukuba, 1-1-1 Tennoudai, Tsukuba 305-8577, Mochida Pharmaceutical Co., Ltd., Pharmaceutical Research Center, 722 Uenohara, Jimba, Gotemba 412-8524,[3] ERATO Environmental Response Project, Japan Science and Technology Corporation, 1-1-1 Tennoudai, Tsukuba 305-8577,[4] Research Center for Advance Science and Technology, The University of Tokyo, Tokyo 153-8904,[5] and SORST, Japan Science and Technology Corporation, Kawaguchi 332-0012,[6] Japan

Received 23 May 2005/Returned for modification 25 June 2005/Accepted 7 August 2005

Occupational and environmental exposure to polycyclic aromatic hydrocarbons (PAHs) has been suggested to provoke inflammatory and/or allergic disorders, including asthma, rhinitis, and dermatitis. The molecular mechanisms of this PAH-mediated inflammation remain to be clarified. Previous studies implied the involvement of PAHs as irritants and allergens, with the reactive oxygen species generated from the oxygenated PAHs believed to be an exacerbating factor. It is also possible that PAHs contribute to the pathogenesis through activation of aryl-hydrocarbon receptor (AhR)-mediated transcription, since PAHs are potent inducers of the AhR. To address this point, we generated transgenic mouse lines expressing the constitutive active form of the AhR in keratinocytes. In these lines of mice, the AhR activity was constitutively enhanced in the absence of ligands, so that any other direct effects of PAHs and their metabolites could be ignored. At birth, these transgenic mice were normal, but severe skin lesions with itching developed postnatally. The skin lesions were accompanied by inflammation and immunological imbalance and resembled typical atopic dermatitis. We demonstrate that constitutive activation of the AhR pathway causes inflammatory skin lesions and suggests a new mechanism for the exacerbation of inflammatory diseases after exposure to occupational and environmental xenobiotics.

A steady increase in the prevalence of allergic diseases has been noted over the last century (30). Exposure to environmental xenobiotics was reported as one of the risk factors associated with the development of atopy and asthma (3). Polycyclic aromatic hydrocarbons (PAHs) are one of major environmental pollutants present in automobile exhaust, cigarette smoke, various foods, and industrial wastes. The skin, respiratory tract, and digestive tract are the first tissues that come into contact with these exogenous chemicals. Recent studies suggested that inhalation of PAHs in diesel exhaust particles and cigarette smoke triggers inflammatory responses in the respiratory tract, resulting in rhinitis and asthma (13, 21, 31, 33). Occupational exposure to PAHs or topical application of chemicals or drugs containing PAHs elicits inflammatory skin diseases, known as contact hypersensitivity or dermatitis (36, 37). In spite of the increasing number of reports showing a relationship between PAHs and inflammatory disorders, the precise molecular mechanisms by which such chemicals contribute to the development of pathological states remain to be clarified.

The carcinogenic and mutagenic effects of PAHs are well documented (for instance, see review in reference 32) and genetic and biochemical studies indicate that most of these responses elicited by PAHs are mediated through binding to aryl-hydrocarbon receptor (AhR) (22), since PAHs are potent inducers of the AhR activity (12). On the contrary, the involvement of AhR in the inflammatory effect of PAHs is controversial, since dioxins, a typical group of ligands for AhR, suppress the allergen-specific immune responses (10, 35) and often induce chloracne, whose clinical and histopathological appearance is rather distinct from those of PAH-mediated contact dermatitis (6, 37). Usually, the latter is accompanied by itching and is associated with inflammation, whereas the former does not display these signs even in the late stages of the disease (6, 37). Instead, the PAHs have been suggested to provoke inflammation as primary irritants or by allergic mechanisms against PAHs or their metabolites (1, 7, 37). Other lines of evidence suggest that reactive oxygen species generated by oxygenated PAHs appear to enhance the allergic response (4, 15). PAHs have also been shown to stimulate an increase in the DNA-binding activity of NF-κB, which in turn induces cytokine gene expression and provokes the allergic response (28).

The effect of environmental xenobiotics on the immune systems has been intensively examined, but uncertainty remains as to whether these compounds do indeed influence immune responses. Difference in the experimental systems seems to

* Corresponding author. Mailing address: Center for TARA, University of Tsukuba, 1-1-1 Tennoudai, Tsukuba 305-8577, Japan. Phone: 81-29-853-7320. Fax: 81-29-853-7318. E-mail: hozumim@tara.tsukuba.ac.jp.

give rise to distinct results. For instance, there is a report showing that PAHs and 2,3,7,8-tetrachlorodibenzo-*p*-dioxin (TCDD) directly enhance the immunoglobulin E (IgE) production when added to the purified B cells (33). Another study showed that TCDD preincubation results in the decrease of IgE production from the B-cell culture (14). This situation convinced us that an integrated in vivo experimental system should be established for evaluating and dissecting the biological effect of these compounds.

We surmised that, in any case, AhR-mediated transcription should be activated in the tissues where the AhR ligands are applied. In order to clarify the contribution of AhR-mediated transcription to the development of inflammatory disorders, we attempted to discriminate between the contribution of the AhR pathway and the other effects of PAHs. Therefore, in the present study, we assessed the direct contribution of the AhR pathway to inflammatory disorders by utilizing the constitutive active form of AhR (AhR-CA) that can activate transcription in the absence of exogenous chemicals. Skin was chosen as the tissue to examine AhR-CA expression because the consequences are easy to observe, and transgenic mice were generated that express AhR-CA in keratinocytes under the regulation of keratin 14 promoter (11). These transgenic mice were normal at birth, but severe skin lesions with itching developed postnatally. The skin lesions were accompanied by inflammation and immunological imbalance and resembled typical atopic dermatitis. This result clearly shows that constitutive activation of the AhR pathway is sufficient to trigger the inflammatory skin lesions and suggests the involvement of AhR-mediated transcription in the inflammatory diseases after exposure to occupational and environmental xenobiotics.

MATERIALS AND METHODS

Generating transgenic mice expressing AhR-CA. Male and female BDF_1 mice were purchased from CLEA Japan (Tokyo) to obtain fertilized eggs for DNA microinjection. AhR-CA transgenic mice, generated as described below, were maintained in the mixed background of C57BL/6 and DBA/2. AhR-CA transgenic mice and their wild-type littermates were housed in plastic cages in an air-conditioned room at a temperature of 24 ± 1°C, a humidity of 55% ± 5%, and a 12-h light-dark cycle.

For the construction of the pK14-AhR-CA-HA transgene, we first made a cDNA fragment encoding the constitutive active form of mouse AhR (AhR-CA) with a hemagglutinin (HA) tag sequence at its 3′ end (pBSK-AhR-CA-HA). The ligand-binding domain (277 to 418 amino acids [aa]) of AhR was deleted to generate AhR-CA. In brief, we generated AhR-CA cDNA by ligating the PCR-amplified fragments that encode the N-terminal (1 to 276 aa) and C-terminal (419 to 805 aa) halves of the AhR with an internal linker sequence (GGGGGA TCGGG), and the resultant cDNA fragment was subcloned into pBluescript II SK(+) vector (pBSK-mAhR-CA). An HA tag sequence was added to the 3′ end to make pBSK-AhR-CA-HA. To construct pK14-AhR-CA-HA, the blunt-ended HindIII/XbaI fragment of the HA-tagged AhR-CA cDNA was subcloned into the blunt-ended BamHI and XbaI sites of a human K14 promoter/enhancer cassette plasmid (a generous gift from E. Fuchs [11]). The construct was linearized, purified, and injected into fertilized oocytes. The transgenic mice were identified by the PCR (ca. 30 to 32 cycles of 94°C for 30 s, 60°C for 30 s, and 72°C for 30 s) with a primer set: 5′-AAC TCT CTG TTC TTA GGC TCA GCG TC-3′ and 5′-ATA CGC TCT GAT GGA TGA CAT CAG ACT-3′. Fluorescence in situ hybridization (FISH) analysis was performed with the splenocytes prepared from Line 234 female mice and the pK14-AhR-CA-HA transgene as a probe through the standard procedure by Trans Animex Co., Ltd. (Hokkaido, Japan).

Immunoblotting analysis. Dorsal skins were homogenized in buffer containing 20 mM HEPES (pH 7.6), 20% glycerol, 10 mM NaCl, 1.5 mM $MgCl_2$, 0.2 mM EDTA, 1% protease inhibitor, 1 mM dithiothreitol, and 1 mM phenylmethylsulfonyl fluoride. Homogenized samples were mixed with an equal volume of gel loading buffer (100 mM Tris-HCl [pH 6.8], 4% sodium dodecyl sulfate, 0.2% bromophenol blue, 20% glycerol, 200 mM dithiothreitol) and then sonicated and boiled at 100°C for 3 min. Soluble fractions were collected as supernatants after centrifugation. An aliquot (40 μg) of each sample was separated by sodium dodecyl sulfate–7.5% polyacrylamide gel electrophoresis and transferred onto Immobilon-P Transfer Membrane (Millipore Corp., Bedford, MA). The membrane was incubated in anti-HA antibody (sc-805; Santa Cruz Biotechnology, CA). The signal was detected using ECL and a Western blotting detection system (Amersham Pharmacia Biotech).

RNA blotting analysis. Total RNA was prepared from dorsal skin by using Isogen (Nippon Gene, Tokyo) according to the manufacturer's instructions. Total RNA (15 μg) was separated by electrophoresis on a 1% formaldehyde-agarose gel and subsequently transferred onto Zeta-Probe GT Genomic Tested Blotting Membrane (Bio-Rad Laboratories, Hercules, CA). The membrane was probed with ^{32}P-labeled CYP1A1 cDNA fragment.

Histological and immunohistochemical analyses. Skins were fixed in 3.7% formaldehyde, embedded in paraffin, and sectioned. For histological analysis, the samples were stained with hematoxylin and eosin. Alcian blue staining was used for detecting mast cell granules. For the detection of CYP1A1, samples were allowed to react with anti-CYP1A1 antibody (sc-9828; Santa Cruz Biotechnology) overnight. Anti-CYP1A1 antibody binding was detected with horseradish peroxidase-conjugated anti-goat IgG antibody and diaminobenzidene was used as a chromogen.

Measurement of grooming duration and scratching frequency. Individual mice were kept in a cage in a calm state and monitored by video camera for 30 min. Grooming duration and scratching frequency were measured over a randomly selected 10-min period. Grooming of any part of the body using the forepaw or mouth was taken as a grooming episode, and a tally was made of the duration of each episode within the 10-min period. A series of scratching behavior using the hind paw was taken as one scratching episode, and the frequency of the episodes were counted for 10 min. Three mice were examined independently at 6 weeks of age.

cDNA microarray analysis. Ten-day-old AhR-CA mice of Line 239 (two males and three females) and their wild-type littermates (two males and two females) were sacrificed, and total RNAs were isolated from their back skin. The isolated RNAs were further purified by RNeasy RNA isolation kit (QIAGEN). Purified RNA was used for preparing labeled cRNA that was hybridized to a mouse expression array 430A gene chip (Affymetrix, Santa Clara, CA). Experimental procedures for GeneChip were performed according to the Affymetrix GeneChip expression analysis technical manual. The results were deposited in the Gene Expression Omnibus (GEO) at the National Center for Biotechnology Information (GEO accession number GSE2955).

cDNA synthesis and reverse transcription-PCR (RT-PCR). Total RNA (3 μg) was reverse transcribed by Superscript II (Invitrogen) with 150 ng of random hexamer at 42°C. Each cDNA was amplified by PCR using ExTaq (TaKaRa Shuzo, Tokyo, Japan). The primers used were 5′-AGT GCA GAC AGT CCA CAG CA-3′ and 5′-TGC TCA GAG TAG TGA CCG AAC G-3′ for CYP1B1, 5′-TCA GTT CCC ATT GCA GTG G-3′ and 5′-TGG AAT GGA CTT GCC C-3′ for NQO1, 5′-ACA CGG TGC TGG ACG AAT C-3′ and 5′-ACG TAC GCC CAG TGA A-3′ for ADH, 5′-TTA CCA TGG GAG CTG AG-3′ and 5′-CCA GAG CGA AGC CAT TGA G-3′ for AhRR, 5′-ACC CGG ACC CAA AAC TTA G-3′ and 5′-TGT TTG CCA GCA GTG ATC-3′ for keratin 1, 5′-TTG AGC AGT ACA TCA GCA A-3′ and 5′-GGA TCA TGC GGT TGA-3′ for keratin 6, 5′-TCA TTA TTG CCA CCC AGG A-3′ and 5′-TCT CCA GGC CCT GGA A-3′ for keratin 16, 5′-TTC CTT GCT TTG GCA TG-3′ and 5′-CAG TTC TGC TTT GGA TC-3′ for CCL20, 5′-CAA CTT TGG CCG ACT TC-3′ and 5′-GAGT GAA CAT TAC AGA TTT ATC CCC-3′ for IL-18, 5′-CTA TCG TGC TCG AAT GAA CAC-3′ and 5′-GCC AAC AGG AAG CTG AGA GT-3′ for HO-1, and 5′-CGA GCA CAG CTT CTT T-3′ and 5′-AGG TAG TCT GTC AGG T-3′ for β-actin.

Measurement of serological parameters. Thirteen AhR-CA mice and twelve wild-type littermates aged 7 to 14 weeks were examined. Blood was drawn from retro-orbital vessels. IgE, IgG1, IgG2a, IgG3, and IgM were quantified by using enzyme-linked immunosorbent assay (ELISA). Cytokine production from spleen T cells stimulated with anti-CD3 monoclonal antibody. We treated 48-well flat-bottom microplates with 2 μg of anti-CD3 antibody (145-2C11; BD Pharmingen) and 0.5 μg of anti-CD28 antibody (PV-1; SBA). Splenocytes were prepared from seven AhR-CA mice and eight wild-type littermates aged from 7 to 14 weeks. A total of 5×10^6 cells were seeded per well and cultured with 1 ml of RPMI 1640 medium supplemented with 10% fetal bovine serum for 24 h. The culture supernatants were then collected and interleukin-2 (IL-2), IL-4, IL-5, IL-12, and gamma interferon (IFN-γ) were quantified with ELISA.

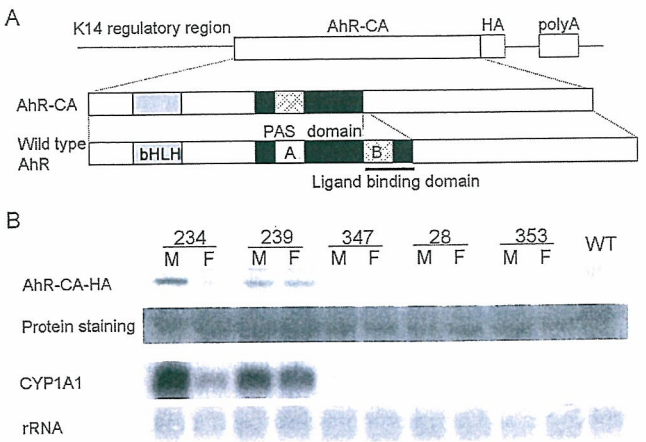

FIG. 1. Generation of AhR-CA transgenic mice. (A) Structure of the transgene. Basic helix-loop-helix (bHLH) and PAS domains are indicated as shaded and dotted boxes, respectively. The PAS-B domain serving as a ligand-binding domain (indicated by a bar) was deleted to generate the AhR-CA molecule. An HA tag was added at the C terminus of the protein. (B) Expression of the transgene correlates with the CYP1A1 mRNA level. HA-tagged AhR-CA was detected by immunoblot analysis with anti-HA antibody. CYP1A1 mRNA was detected by RNA blot analysis. The corresponding line numbers are shown at the top. M, male; F, female; WT, wild type.

RESULTS

Generation of transgenic mouse lines expressing AhR-CA in keratinocytes and integration of transgene into X chromosome in one of the lines. In order to explore the possibility that activation of the AhR pathway can elicit inflammatory response in vivo, we generated transgenic lines of mice that express AhR-CA in keratinocytes under the regulation of the keratin 14 (K14) promoter (Fig. 1A). Among several lines of mice generated, two (Lines 234 and 239) were found to express the AhR-CA transgene at high levels (Fig. 1B). Since the expression of AhR-CA in female Line 234 mice was consistently weaker than that in male mice of Line 234, we mapped the chromosomal localization of the transgene by using FISH analysis. The result unveiled that the transgene was integrated into the X chromosome in Line 234 (data not shown). Thus, we suspected that the transgene was subjected to random inactivation of the X chromosome (i.e., lionization [29]) and that the female skin was composed of two kinds of keratinocytes, the cells expressing the transgene and the cells whose transgenes were silenced, consequently resulting in the lowered expression of AhR-CA in female mice compared to male mice when the whole skin was examined.

Since the male mice of Line 234 died before weaning (data not shown), an essential gene on the X chromosome must have been disrupted by integration of the transgene. Line 234 mice, especially female mice, were found to provide strong evidence for a link between activation of the AhR pathway and the development of inflammatory lesions as will be described below. The abundance of AhR-CA showed a good correlation with the abundance of CYP1A1 mRNA, one of the target gene products of the AhR (Fig. 1B), demonstrating that AhR-mediated transcription is activated in the skin of the transgenic mice without any exogenous stimuli.

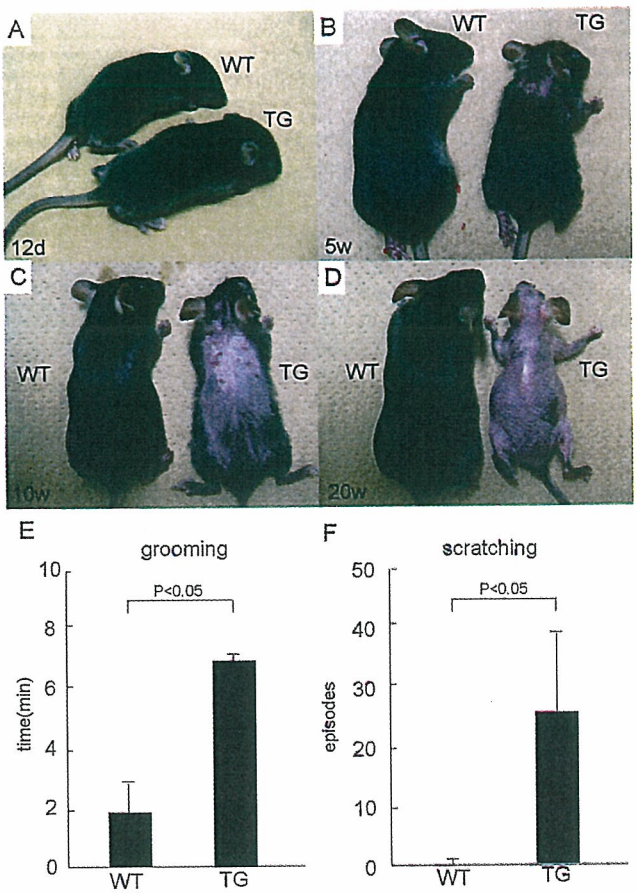

FIG. 2. Macroscopic observation of Line 239 mice. (A) Twelfth day after birth. Note that skin lesions are not apparent. (B) Fifth week. An eczematous change emerges on the back skin. (C) Tenth week. Erosive dermatitis with crusts is observed. (D) Twentieth week. Note that re-epithelialization follows, and the fur coat is completely lost. (E and F) Observation of behaviors related to skin itching. The total duration of grooming behavior within 10 min was measured for three independent mice, and the averages and standard deviations are shown in panel E. The frequency of scratching episodes within 10 min was counted for three independent mice, and the averages and standard deviations are shown in panel F. The differences between the AhR-CA mice (TG) and the wild-type control mice (WT) are statistically significant ($P < 0.05$).

AhR-CA transgenic mice postnatally develop skin lesions with itching. Whereas Line 239 mice were normal at birth and healthy up to 12 days of age (Fig. 2A), they gradually developed erosive eczema in the back skin by 3 to 5 weeks after birth (Fig. 2B). Eventually, a massive loss of their fur coats occurred after the tenth week, even under specific-pathogen-free conditions (Fig. 2C and D). The whole skin over the body was subjected to the same process of skin lesion development. We noticed that both female and male mice of Line 239 frequently scratched their skin, which started around the time of weaning. Closer examination with the video tape recording revealed that both male and female transgenic mice of Line 239 performed grooming for longer periods of time and scratched much more frequently than their wild-type littermates (Fig. 2E and F). An important observation was that, although the transgene was already expressed in the embryos of the late fetal stage (data